JGR Planets

RESEARCH ARTICLE
10.1029/2020JE006696

High-Temperature VIS-IR Spectroscopy of NH_4-Phyllosilicates

S. De Angelis[1], M. Ferrari[1], M. C. De Sanctis[1], E. Ammannito[2], A. Raponi[1], and M. Ciarniello[1]

[1]INAF-IAPS, Rome, Italy, [2]ASI - Agenzia Spaziale Italiana, Rome, Italy

Key Points:

- Reflectance spectra of NH_4-phyllosilicates measured in the 0.35–5 μm range, in high vacuum and at temperatures up to 723 K
- Ammonium band at 3.1 μm is almost completely lost in the temperature range 623–723 K
- Spectra of dehydrated NH_4-phyllosilicates compared with Ceres infrared data from Dawn mission; 3-μm band in NH_4-saponites above 623 K can match with Ceres spectrum

Correspondence to:

S. De Angelis,
simone.deangelis@inaf.it

Citation:

De Angelis, S., Ferrari, M., De Sanctis, M. C., Ammannito, E., Raponi, A., & Ciarniello, M. (2021). High-temperature VIS-IR spectroscopy of NH_4-phyllosilicates. *Journal of Geophysical Research: Planets*, *126*, e2020JE006696. https://doi.org/10.1029/2020JE006696

Received 16 SEP 2020
Accepted 7 MAY 2021

Author Contributions:

Conceptualization: S. De Angelis, M. Ferrari, M. C. De Sanctis, E. Ammannito
Data curation: S. De Angelis, A. Raponi, M. Ciarniello
Formal analysis: S. De Angelis, A. Raponi, M. Ciarniello
Funding acquisition: M. C. De Sanctis
Investigation: S. De Angelis, M. Ferrari, A. Raponi, M. Ciarniello
Methodology: S. De Angelis, M. Ferrari, E. Ammannito
Project Administration: M. C. De Sanctis, E. Ammannito
Resources: S. De Angelis, M. Ferrari
Software: S. De Angelis

Abstract Ammonium phyllosilicates have been identified on the dwarf planet Ceres, thanks to infrared telescopic and orbital data from the Dawn mission, by means of the 3.06 μm spectral feature. Nevertheless, it is not known which ammonium-bearing phyllosilicate species are present, nor the thermal processing they underwent throughout Ceres history. Identifying the NH_4^+-hosting mineral species is important for deciphering Ceres' surface mineralogy, which provides a link to its interior and putative different evolutionary pathways. Ammoniated species can have formed in the presence of water/ammonia-rich fluids in different conditions in the interior of the planet; in case of an exogenous outer Solar System origin, they can have undergone heating at depth. In this work, we study the visible-infrared spectra of several NH_4-treated/untreated phyllosilicates in the range 0.35–5 μm, acquired in vacuum and at temperatures between 298 and 723 K. Previously NH_4-phyllosilicates have been mostly studied at ambient condition, preventing the characterization of the NH_4^+ band at 3.06 μm, due to overlapping bands of water. With this new set of measurements, we investigate how the NH_4-phyllosilicates spectra are modified when the mineral's water is lost, and which temperature is the limit for the releasing of NH_4^+. We present the first high-temperatures/high vacuum 3-μm reflectance spectra of ammonium phyllosilicates. Our measurements indicate that Mg-phyllosilicates are the best candidates for the ammonium-bearing species. Moreover, the almost complete disappearing of NH_4^+ absorption feature at ~3.06 μm for ammoniated phyllosilicates heated at the highest temperatures indicates that such species on Ceres could not have experienced temperatures higher than 623 K.

Plain Language Summary Hydrated/ammonium minerals have been observed on Ceres thanks to the Dawn mission instruments. This indicates that Ceres accreted volatile materials and ammonia from the outer Solar System during its formation. Ammonium minerals are observed with spectrometers on Ceres, thanks to the sunlight they reflect in the visible-infrared interval. The spectrum of such minerals, the way they absorb light at different frequencies, depends on physical parameters such as composition, temperature, pressure, radiations. Different types of phyllosilicates could host ammonium, with implications for the thermal evolution of the planet. It is not well constrained which the hosting species is, nor the maximum temperature it underwent, or the formation environment. It is important to characterize in laboratory such materials in various conditions that can simulate the ambient on Ceres' surface. Here we investigated in laboratory, the visible-infrared spectra of hydrated-ammonium minerals, subject to different experimental conditions; we studied minerals in vacuum and at high-temperatures, with the aim of removing water from the minerals for a better comparison with mission data. Data acquired in laboratory on dehydrated samples will be helpful for comparison with data from missions, in order to identify the ammonium minerals and to give clues on the thermal evolution of Ceres.

1. Introduction

The presence of ammonium-bearing minerals on the surface of (1) Ceres has been first suggested by King et al. (1992), using ground-based spectral data. After that, NH_4-phyllosilicates have been advocated as one of the main constituents of the Ceres surface (Ammannito et al., 2016; De Sanctis, Ammannito, et al., 2015), interpreting to the spectra acquired by the VIR spectrometer (De Sanctis, Coradini, et al., 2011) onboard the Dawn spacecraft (C. T. Russell et al., 2004). The Ceres spectra in the range of 1–5 μm have shown a clear signature at 3.06–3.07 μm, assigned to NH_4-phyllosilicate. Nevertheless, the specific phyllosilicates bearing ammonium were not fully constrained, also due to the limited availability of NH_4^+-phyllosilicate spectra acquired in the laboratories (Berg et al., 2016; Bishop, Banin, et al., 2002; Ehlmann et al., 2018; Ferrari et al., 2019; Krohn & Altaner, 1987). Moreover, the NH_4^+-phyllosilicate measurements were usually acquired in the ambient conditions, which are very different from the pressure and temperature conditions at

Supervision: M. C. De Sanctis, E. Ammannito
Validation: S. De Angelis, M. C. De Sanctis, E. Ammannito
Visualization: M. C. De Sanctis, E. Ammannito, A. Raponi, M. Ciarniello
Writing – original draft: S. De Angelis, M. Ferrari, M. C. De Sanctis

the Ceres surface. Thus, the identification of the ammonium-bearing species present on Ceres is not straightforward. On Earth, ammoniated minerals occur naturally in a variety of geological settings and, in many of these cases, the nitrogen is supplied by the decomposition of organic material. In hydrothermal settings, NH_3 gases or NH_4-rich aqueous solutions can exchange ammonium with interlayer cations in clay minerals (e.g., Blake, 1965). However, NH_4^+ can be part of the phyllosilicate mineral lattice (as an interlayer cation) or can be adsorbed on the mineral surface. Spectral data of ammonium-bearing minerals and rocks have been previously reported (e.g., Berg et al., 2016; Bishop, Banin, et al., 2002; Ehlmann et al., 2018; Farmer & Russell, 1967; Ferrari et al., 2019; Knop, Oxton, & Falk, 1979; Knop, Westerhaus, & Falk, 1980; Knop, Westerhaus, Falk, & Massa, 1985; Krohn & Altaner, 1987; Pironon et al., 2003) and show features related to the presence of nitrogen complexes at 1.56, 2.05, 2.12, 3.06, 3.25, 3.55, 4.2, 5.7, and 7.0 μm (Bruno & Svoronos, 1989; Robinson, 1974). Some of these spectra have been used in spectral models to retrieve the minerals present on the Ceres surface (e.g., De Sanctis, Ammannito, et al., 2015; Marchi et al., 2019; Raponi et al., 2019). However, such models do not unambiguously identify the NH_4^+ carriers mostly because the spectra available in the literature have been acquired at pressure-temperature (P-T) conditions extremely different from the conditions at Ceres' surface. Previous spectroscopic studies of clays and ammoniated clays at high-temperatures generally were focused on the mid-infrared spectral range (the region around 1,400 cm^{-1}) and in most cases, they are in absorbance or in transmission mode (Che et al., 2011; Farmer & Russell, 1967; J. D. Russell & Farmer, 1964; J. D. Russell & White, 1966; Yang et al., 2017; Yariv, 2001). Here, we obtain, purify, and ammoniate a variety of Ceres-relevant analog materials. The spectra of the ammoniated phyllosilicates have been acquired in reflectance in several different P-T conditions, with the aim to produce laboratory spectral data more consistent with the conditions that materials may have experienced at Ceres deep in the crust. In fact, although the Ceres surface maximum temperature is of the order of ∼230–240 K (Formisano et al., 2015), nevertheless the average spectrum as measured by VIR may carry the record of the high-temperature thermal processing the materials have undergone in the crust, especially in the ∼3 μm region.

2. Materials and Methods

The aim of this work is to measure ammoniated phyllosilicates in various conditions of pressure and temperature. Particular attention was given to the dehydration of the ammoniated minerals. In fact, most of the previous spectral measurements of ammoniated phyllosilicates show clear signs of residual water used in the preparation of the samples and the absorbed water from the ambient. In these experiments, we tried to measure the spectra in hydration conditions similar to those expected on the Ceres surface.

2.1. Samples

2.1.1. Samples Description and Preparation

Natural phyllosilicates and NH_4-phyllosilicates produced in the laboratory at INAF-IAPS have been used for this experiment. The natural samples have been purchased on the market by the Clay Minerals Society (CMS) and Minerals Unlimited; these are listed in Table 1. The ammoniated samples have been produced in our laboratory, starting from the natural phyllosilicates from CMS and Min.Unlim., according to a procedure modified after Bishop, Banin, et al. (2002), and are listed in Table 1. The detailed description of the experiment concerning the production of NH_4-phyllosilicates and VNIR/mid-IR measurements at room P-T is reported in Ferrari et al. (2019), for five of the samples. Both VNIR and mid-IR (2–20 μm) measurements on untreated, NH_4-treated and NH_4-treated + leached samples demonstrated that the NH_4^+-injection procedure was successful. All the samples, before the treatment with ammonia, have been produced in the form of fine powder (grain size $d < 36$ μm), by means of grinding and dry sieving, starting from the raw minerals as coarse fragments. The procedure of the treatment with ammonia is carried out by keeping the minerals in liquid NH_3-H_2O solutions (33 vol%) and then by drying the solution and extracting the solid phase. After this treatment the clay minerals particles tend to re-aggregate, thus it was necessary to proceed with further grinding without additional sieving. Finally, we can reasonably assume that ammoniated grains are characterized by a size $d < 50$ μm: this particle size was assumed on the basis of the sieve diameter. For each sample, both raw and ammoniated, three separate equal aliquots were produced to be measured with two different instruments for spectral analyses and

Table 1
Samples Used in This Work

Sample	Id#	Source	Description
Beidellite	Beid	Min.Un.	Al-rich dioctahedral smectite; Al^{3+} in octahedral sites and Si^{4+}/Al^{3+} in tetrahedral positions; has isomorphic substitutions mainly within T layers
Illite-smectite	ISCz1	CMS	K-rich Dioctahedral mineral; interlayer space is mainly occupied by K^+ or sometimes by NH_4^+; in illite interlayer space is non-hydrated and not expandable
Nontronite-green	NAu1	CMS	Fe-rich dioctahedral smectite; Fe^{3+} in octahedral sites; Al^{3+} and Fe^{3+} substitutions for Si^{4+} in tetrahedral sites
Nontronite-brown	NAu2	CMS	Fe-rich dioctahedral smectite; Fe^{3+} in octahedral sites; Al^{3+} and Fe^{3+} substitutions for Si^{4+} in tetrahedral sites
Saponite	SapBaj	Min.Un.	Fe-rich/Mg-rich trioctahedral smectite; Al^{3+} for Si^{4+} substitutions in T layers; Al^{3+}-Mg^{2+} substitutions in O layers
Saponite	SapBar	Min.Un.	Mg-rich trioctahedral smectite; Al^{3+} for Si^{4+} substitutions in T layers; Al^{3+}-Mg^{2+} substitutions in O layers
Montmorillonite	SCa3	CMS	Al-rich dioctahedral smectite; Al^{3+} in octahedral sites and Si^{4+}/Al^{3+} in tetrahedral positions; has isomorphic substitutions mainly within O layers (Al^{3+} for Mg^{2+} and Fe^{3+})
Hectorite	SHCa1	CMS	Mg-rich trioctahedral smectite; Mg^{2+} in octahedral sites, often with Li^+ substitutions

Abbreviation: CMS, Clay Minerals Society; Min.Un., Minerals Unlimited.
Note. Farmer (1974) and Madejovà et al. (2017).

for chemical characterization (see Section 2.2). It must be noted that the ammoniated samples are produced in aqueous solutions and, for this reason, their spectra, acquired in ambient conditions, typically show the bands due to the water used in the solutions (Ferrari et al., 2019). Although we did not measure real "blank" samples (i.e., samples treated with the same protocol but only water), in additional laboratory tests on five samples, concerning re-hydration in air after dehydration, we verified that such phyllosilicates become almost saturated in water just after a few minutes of exposition, as indicated by the very quick increase of the 3-μm band. The samples Beidellite, SapBaj and SapBar and their corresponding ammoniated-phases were not previously measured in the Ferrari et al. (2019) study. In particular the saponite SapBaj specimen resulted slightly naturally ammoniated, as evidenced from IR bands appearing at 1.55 (weak), 2.01, 2.12, and 3.1 μm during preliminary control measurements. Thus, we treated this particular sample in two distinct ways. For the measurements in the range 0.35–2.5 μm (Sections 2.3.1 and 3.2) we used the naturally ammoniated sample. Then, we heated this sample at high-temperature (723 K for 11 days) in order to remove as much ammonium as possible from the sample, without producing mineral alteration. With such a process, we obtained a non-ammoniated specimen of SapBaj, and subsequently, we produced an aliquot of NH_4-SapBaj, according to the procedure described in Ferrari et al. (2019). Finally, we used these two last aliquots for measurements in the 1–5 μm range (Sections 2.3.2 and 3.3). Some samples (e.g., hectorite SHCa1) contained naturally carbonates, as evidenced by IR spectra and by literature data (Che et al., 2011; Earnest, 1983a, 1983b).

2.2. Experimental Setup

2.2.1. XRPD Characterization

The mineralogical characterization of the samples, both phyllosilicates and NH_4-phyllosilicates, have been performed by means of X-Ray Powder Diffraction analyses. The XRPD analyses have been carried out at the University of Bari, Earth Sciences Department (Italy). Diffraction data have been acquired by means of a Rigaku-Miniflex II Diffractometer, using as source the Cu-Kα line radiation (30 kV, 15 mA) at 1.54 Å wavelength. Diffractograms were acquired performing a scan in the 2θ 3°–70° range, with a velocity of 2°/min and 0.02° step. Beam reducing slits of 1.25°, 0.3 mm and 1.25° have been used.

2.2.2. VNIR Setup (Fieldspec): 0.35–2.5 μm

Spectral reflectance measurements in the VIS-NIR range (0.35–2.5 μm) were performed with the ASD Fieldspec-4 setup in use at IAPS/C-Lab, equipped with an environmental cell (De Angelis, Ferrari, De Sanctis, Biondi, et al., 2018; De Angelis, Manzari, et al., 2017). The setup consists of a commercial spectrometer coupled with a Quartz-Tungsten-Halogen light source. The QTH lamp illuminates the sample through an optical fiber, with 100 W power and a 10-mm spot on the sample, placed at a distance of about 5 cm. The illumination angle is about 30° with respect to the normal to the sample surface. An optical fiber bundle collects the reflected light from the sample at zero-emission angle (normal) and carries the signal to the spectrometer. The spectral sampling is 1 nm, the spectral resolution 3–8 nm across the range.

2.2.3. IR Setup (SPIM): 1–5 μm

Spectroscopic reflectance measurements in the IR range (1–5 μm) were carried on with the SPIM facility at IAPS/C-Lab. The details of the setup are described in Coradini et al. (2011) and De Angelis, Ammannito, et al. (2015). The facility consists of an imaging spectrometer that is a spare of the VIR instrument onboard the Dawn spacecraft (De Sanctis, Coradini, et al., 2011). The setup is constituted by (a) an illumination system and sample compartment on an optical bench in air and (b) a detection system inside a Thermo-Vacuum Chamber (TVC). In the standard conditions of measurements, the sample is placed in air on a motorized XYZ-stage. The spectrometer in Offner configuration comprises a 9×0.038 mm^2 entrance slit, a convex grating, a spherical mirror, a flat mirror, and two focal planes: a CCD (0.4–1 μm) and a HgCdTe (1–5 μm). The spectrometer, VIS and IR detector need to be cooled down respectively to 130, 150, and 80 K by means of liquid nitrogen and in high vacuum. A three-dimensional data cube is built, with two spatial dimensions (horizontal X-Y plane) and a third spectral dimension (wavelengths), by translating the sample at specific steps and acquiring consecutive images of the slit. The spatial resolution on the sample is 38 μm/pixel, and the spectral sampling is 2 nm in the VIS and 10 nm in the IR. For our purposes, we only used the IR light source and the IR detector; the setup was equipped with a dedicated environmental chamber, described in the next section. Two samples (NH_4-beidellite and NH_4-SapBaj) have been measured at room P-T conditions with an FT-IR Bruker interferometer, in the 1–5 μm range, using a MCT detector, with 4 cm^{-1} spectral resolution.

2.2.4. P-T Cell

In order to carry on spectroscopic measurements at controlled conditions of pressure-temperature (P-T), we used a P-T chamber developed in our laboratory (De Angelis, Ferrari, De Sanctis, Biondi, et al., 2018). This environmental cell permits to acquire reflectance spectra of samples under different controlled P-T and atmospheric conditions, in particular in high vacuum and at high-temperatures. High vacuum, down to $P = 10^{-7}$ mbar, is obtained through a primary rotary pump and a secondary turbomolecular pump. The powder sample to be measured is placed horizontally within a stainless steel cup, below which a ceramic heater allows increasing the temperature up to 673 K. A thermocouple embedded within the ceramic heater and a PID controller permits to measure the temperature and change the set point. The sample cup, which is about 12 mm high, is in direct contact with the heater, and the sample thermalization occurs in a few minutes, thus we can assume a sample temperature accuracy <5 K with respect to the value measured by the thermocouple. A CaF_2 viewport permits to illuminate the sample and collect the reflected light in a broad range from the visible to the mid-infrared, by means of an external optical system. With the aim of performing our experiments in the different spectral ranges, we equipped both setups (FieldSpec or SPIM) with this cell.

2.3. Spectral Measurements Procedure

2.3.1. VNIR Measurements

Spectra with FieldSpec in the VNIR (<2.5 μm) were acquired upon heating the samples directly in the cell, a few minutes for each temperature. Overtone hydration bands in this spectral range (near 1.5 and 2 μm) rapidly change and reduce greatly with decreasing pressure and increasing temperature, allowing the separation and

Table 2
Spectral Measurements Performed on the Samples

	FieldSpec + cell				SPIM + oven + cell			
Sample	423 K	523 K	593 K	623 K	423 K	523 K	623 K	723 K
Beid					X(°)	X(°)	X(°)	X(°)
ISCz1					X(°)	X(°)	X(°)	X(°)
NAu1					X(°)	X(°)	X(°)	X(°)
NAu2					X(°)	X(°)	X(°)	X(°)
SapBaj					X(°)	X(°)	X(°)	X(°)
SapBar					X(°)	X(°)	X(°)	X(°)
SCa3					X(°)	X(°)	X(°)	X(°)
SHCa1					X(°)	X(°)	X(°)	X(°)
NH_4-Beidellite	X	X	X	X	X(°)	X(°)	X(°)	X(°)
NH_4-ISCz1	X	X	X		X(°)	X(°)	X(°)	X(°)
NH_4-NAu1	X	X	X		X(°)	X(°)	X(°)	X(°)
NH_4-NAu2	X	X	X		X(°)	X(°)	X(°)	X(°)
NH_4-SapBaj	X	X	X	X	X(°)	X(°)	X(°)	X(°)
NH_4-SapBar	X	X	X		X(°)	X(°)	X(°)	X(°)
NH_4-SCa3	X	X	X		X(°)	X(°)	X(°)	X(°)
NH_4-SHCa1	X	X	X		X(°)	X(°)	X(°)	X(°)

Note. The symbol "°" indicates heating in the oven.

clear detection of NH_4^+ bands. To estimate the contribution of the cell window, we acquired a spectrum of the sample at room P-T conditions, with and without the viewport. These measurements also provide the spectrum for the material at room condition. The reference (Spectralon) was measured outside the cell. Typically the window contribution was an attenuation of the signal of <10%, and in rare cases, depending on material brightness, two reflection artifacts appeared in the 1–1.3 μm region. These artifacts, when present, did not influence the absorption bands of interest. In the next section, the procedure for correction for window contribution is described. After the first acquisition, the pumping system was switched on and subsequent data acquisition started once the pressure in the cell stabilized at the limit vacuum. The limit pressure is influenced by the hydration state of the sample, and typically 10^{-4}–10^{-5} mbar were reached with highly hydrated samples in a few tens of minutes. Once a high vacuum was produced in the cell, temperature ramps were carried on at 50 K-steps in the range 298–673 K. Spectra were acquired at each temperature after a few minutes for thermalization.

2.3.2. IR Measurements

In order to acquire spectra in the IR (SPIM setup), ammoniated and non-ammoniated samples were previously heated in an oven for one week at each of the temperatures 423, 523, 623, and 723 K in order to remove adsorbed water and then, at higher temperature, ammonium. This is because while hydration bands in the VNIR rapidly decrease as temperature increases, the 3-μm band needs much longer heating time to appreciate variations. In fact, this band is more sensitive to even a small quantity of hydration. Indeed the 3-μm band complex still remains very intense also for a water content <<1wt% (Salisbury & Walter, 1989). After each of the week-long heating sessions, the spectra of both phyllosilicates and NH_4-phyllosilicates were then acquired in the P-T cell in high vacuum at 323 K, in order to quickly remove any additional humidity adsorbed on the samples once extracted from the oven. The reference target (Infragold) was measured in air outside the cell. No particular artifacts occurred in this range due to the window. The background signal, with a shutter on the lamp, was acquired at the same temperature as for the sample (Table 2).

2.4. Data Processing

2.4.1. VNIR Processing

Data are corrected for the contribution of the CaF_2 window with the following method. The signal S_m measured from the sample within the cell is given by:

$$S_m = T_W \times S_{0c} + S_W$$

in which S_{0c} is the signal from the sample outside the cell (i.e., without window), T_W is the optical transmission of the CaF_2 window (data from the builder company), and S_W is the signal contribution due to the window. The quantity S_W was evaluated for each sample by acquiring at room P-T the spectrum both with and without the cell window. The term S_W could contain some stray light or reflection contribution from the particular sample, depending on its surface brightness or roughness. Thus, the corrected signal at each P-T condition was then obtained by:

$$S_{0c} = \frac{(S_m - S_W)}{T_W}$$

Calibrated reflectance data were obtained by dividing the raw signal, in digital numbers (DN), from the sample by the raw signal from the reference target, after subtracting dark from both signals.

2.4.2. IR Processing

Spectra in the IR were recorded without moving the motorized sample-holder, so at each P-T condition, a line (single slit image) was acquired, consisting of 270 px aligned on the sample. The signal was averaged along the 270 px. The reference target (Infragold) was acquired outside the cell. Reflectance spectra were obtained by ratioing the sample signal and the reference signal, each divided by the respective integration time. The background signal was measured putting a shutter in front of the IR lamp and then subtracted from the above signals.

3. Results

3.1. XRPD Analyses

In all the analyzed samples a shift of the diffraction peak related to 001-plane, toward larger 2θ values, is observed in the NH_4-treated samples, with respect to the untreated samples. These results indicate that the injection of the NH_4^+ ion in the interlayer indeed produces a reduction of the interplanar distance d_{001}. This is due to the fact that the ammonium ion can establish several hydrogen bonds with oxygen from the surface of the smectite layers. The formation of these hydrogen bonds can reduce the swelling of the interplanar space (Diaz Pinthier, 1999). This confirms that the ammoniation procedure was successful and exclude that the NH_4-acetate molecule was incorporated (Ehlmann et al., 2018).The results of the XRPD analyses are reported in Table 3. Most of the samples contain quartz as an accessory mineral, while two of them (saponite SapBar and hectorite SHCa1) also contain carbonates (calcite and/or dolomite). A couple of samples also contain iron oxides (illite/smectite ISCz1, saponite SapBaj).

3.2. VNIR: 0.35–2.5 µm

Spectra acquired with FieldSpec set up in the 0.35–2.5 µm range are shown in Figures 1–6. In Figure 1 examples of spectra, acquired in high vacuum ($<10^{-4}$ mbar) and at room temperature, for two samples (SCa3 and SHCa1 and their corresponding ammoniated-phases) are shown, with the aim of making clear the spectral differences induced by NH_4^+ in this range. In Figures 2–6 for each NH_4-sample, we report the spectra measured at room temperature for decreasing pressures (top panel) and then the spectra measured in high vacuum at increasing temperatures (bottom panel). To be noted that most of the spectra acquired at the highest temperatures are affected by thermal emission above 2 µm.

Table 3
XRPD Analyses Performed on the Phyllosilicates and NH_4-Phyllosilicates: The Interplanar Distance (d_{001}, in Angstrom) for Untreated and NH_4-Treated Samples is Reported

Sample	Id#	Source	d_{001} (Å)	d_{001}-NH_4 (Å)	Main accessory minerals
Beidellite	Beid	Min.Un.	14.71	11.77	Quartz
Illite-smectite	ISCz1	CMS	11.47	10.70	Quartz, feldspar, kaolinite, and goethite
Nontronite-green	NAu1	CMS	14.71	13.58	Kaolinite, quartz, and biotite
Nontronite-brown	NAu2	CMS	13.79	9.81	Quartz and plagioclase
Saponite	SapBaj	Min.Un.	12.33	11.77	Plagioclase and Fe-oxide
Saponite	SapBar	Min.Un.	12.61	11.62	Calcite and dolomite
Montmorillonite	SCa3	CMS	16.05	12.26	Quartz
Hectorite	SHCa1	CMS	12.26	12.18	Quartz, calcite, and dolomite

Note. Main additional accessory minerals are also listed in the right column.

3.2.1. NH_4-Beidellite

The spectra of ammoniated beidellite are displayed in Figure 2 (left panels). The room P-T spectrum (Figure 2a) is characterized by hydration features near 1.4 and 1.8 and 1.9 μm. A unique NH_4^+ absorption is visible at 2.1 μm (vertical line); the 2.21-μm feature is likely due to Al-OH (Clark et al., 1990). The visible range is characterized by a strong red slope below 1 μm and by a weak and large absorption near 0.6 μm, perhaps due to Fe^{3+}. After pumping, the hydration features at 1.4–1.9 μm reduce greatly, and two very weak NH_4^+ absorptions appear at 1.55 and 2.01 μm. In high vacuum spectra, the NH_4^+ features at 1.55 and 2.01 μm are well-separated from the neighbor hydration bands occurring at 1.4 and 1.9 μm. Upon raising the temperature the hydration bands become even smaller. The ammonium absorptions do not vary notably in depth and area in the 323–600 K temperature range. Depth and area start to decrease considerably above 623 K (Figure 7).

3.2.2. NH_4-Illite-Smectite ISCz1

Ammoniated illite-smectite ISCz1 spectra are shown in Figure 2 (right panels). The chemical composition of the raw non-ammoniated sample is reported in Gailhanou et al. (2007), indicating this sample contains mainly the cations Al^{3+}, Mg^{2+}, and lower quantities of Fe^{2+}/Fe^{3+} and Ti^{2+}. Iron is responsible for the absorptions at 0.5 and 0.92 μm. Features at 2.2, 2.31, and in the 2.4-μm region are due to Al-OH and Mg-OH. At ambient temperature and pressure, the 1.55 and 2.01-μm absorptions are completely hidden within the hydration bands, while the 2.1 μm is slightly visible; all the three ammonium bands become clearly discernible and separate after pumping to high vacuum, below 10^{-2} mbar. After heating, these features remain quite stable until 523 K.

3.2.3. NH_4-Nontronite NAu1

The spectra are shown in Figure 3 (left panels). In the spectrum acquired at room P-T (rPT), the bands occurring near 0.65 and 0.95 μm are due to Fe^{3+} content (3.68 wt%) in this iron-smectite (Che et al., 2011; Clark et al., 1990). The features appearing at 2.21, 2.24 and 2.29 are related to Al-OH, Mg-OH and Fe-OH, although the Mg content in the sample is very low (Che et al., 2011). A noisy feature visible near 2.4 μm is likely due to Al-OH. The bands due to NH_4^+ ion are located at 1.55, 2.01 and 2.12 μm, indicated by vertical lines in the plots. It can be noted that in the spectrum at room P-T, the ammonium bands are weak and embedded within the OH/H_2O bands occurring near 1.4 and 1.9 μm. After pumping down to about 10^{-6} mbar (Figure 2a), much of the adsorbed water is removed and the hydration bands become narrower, permitting the identification of two ammonium features as separate and clearly visible. The effect of pumping results in the removal of the hydration absorptions at longer wavelengths in the 1.4 and 1.9-μm band complexes, which are related to weakly bound water (Bishop & Pieters, 1995; Bishop, Pieters, & Edwards, 1994). During the temperature increase stage (Figure 2c) the ammonium bands get even more separate and discernible. Above ∼537 K the continuum due to thermal emission begins to increase at wavelengths >2 μm, affecting the spectra at high-temperatures.

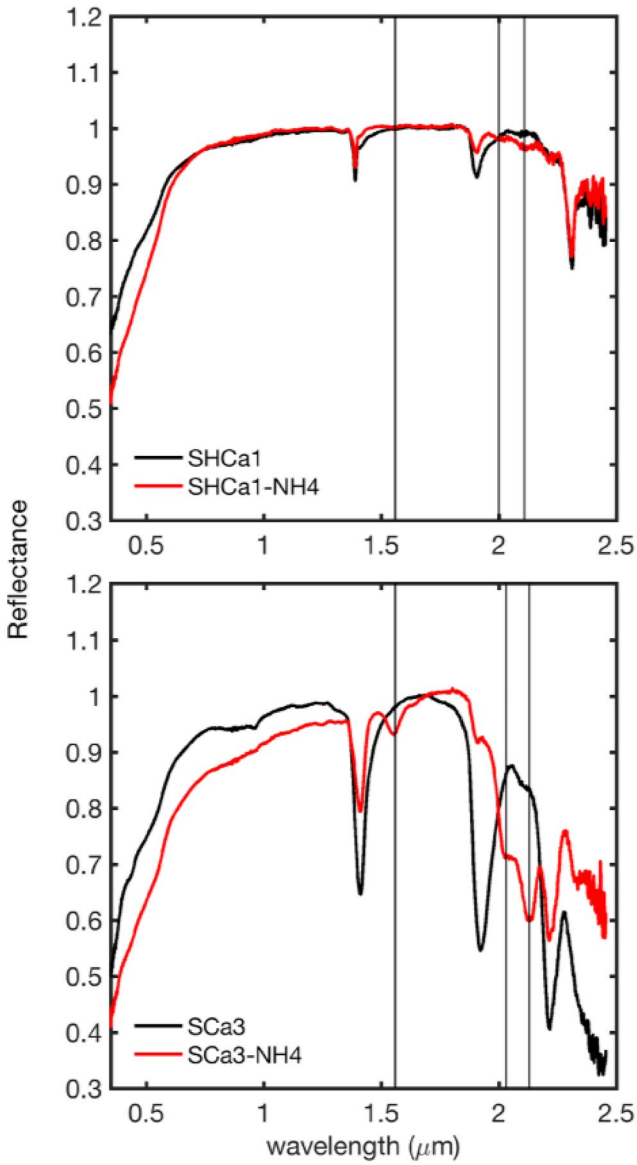

Figure 1. Example spectra of two samples (SHCa1, top, and SCa3, bottom; black) and their corresponding ammoniated-phases (red). Spectra have been acquired at room temperature in vacuum (<10^{-4} mbar). The vertical lines indicate the presence of the three ammonium features occurring in this spectral range.

3.2.4. NH_4-Nontronite NAu2

The spectra of NH_4-NAu2 are displayed in Figure 3 (right panels). This Fe-smectite is similar to the previous one, although with a little more iron content (3.83 wt%) and with a very low Mg content (Che et al., 2011). The spectra show Fe^{3+} absorptions at 0.65–0.95 μm. Features at 2.24, 2.29, and 2.4 μm are attributed to Al-OH, Fe-OH, and Al-OH (Clark et al., 1990). The ammonium bands occur at 1.55, 2.01, and 2.12 μm. In the rPT spectrum, the 1.55 and 2.01-μm features appear embedded in the 1.4 and 1.9-μm hydration bands. By removing adsorbed water after pumping, 1.55 and 2.01-μm absorptions become clearly evident. In this case, they are weaker than in the NH_4-NAu1 sample. The 1.55 and 2.01-μm features start to appear as separate bands when the pressure drops below about 10^{-2} mbar. After heating, the ammonium absorptions remain nearly constant for the different heating steps, although the 2.01–2.12-μm bands tend to become less separate for $T > 473$ K. Also in this case, for $T > 473$ K, the continuum due to thermal emission increases above 2 μm, affecting the spectra at high-temperatures.

3.2.5. NH_4-Saponite SapBar

Spectra of ammoniated saponite NH_4-SapBar are displayed in Figure 4. They are characterized by absorption features due to hydration located at 0.95, 1.16, 1.4, 1.79, and 1.9 μm. The 1.4-μm band complex has absorptions at 1.39, 1.42, and 1.46 μm. The 1.9-μm complex comprises the absorptions at 1.91 and 1.97 μm. The band at 2.31 (and maybe the one at 2.39 μm) is due to Mg-OH. The features attributed to ammonium occur at 1.55, 2.02, and 2.12 μm. The 1.55 and 2.02-μm absorptions are masked by hydration and become very clear and discernible in high vacuum, below 10^{-2} mbar. During the heating stage, the NH_4^+ bands are almost stable and start to decrease in intensity above 523 K. The spectrum at 593 K is affected by the thermal emission.

3.2.6. NH_4-Montmorillonite SCa3

Spectra of ammoniated montmorillonite SCa3 are displayed in Figure 5 (left panels). Che et al. (2011) report the chemical composition and structural formula of this sample, which contains mainly Al^{3+} and Mg^{2+} cations and Fe^{3+} in trace amounts. Iron is responsible for the very weak and broad absorptions near 0.55 and 1 μm. Water and OH are responsible for the absorptions at 0.97, 1.16, 1.42, 1.79, and 1.91 μm, while the 2.21-μm feature is related to Al-OH. The ammonium features occur at wavelengths 1.55, 2.02, and 2.13 μm. As for the other samples, the 1.55 and 2.02-μm, at ambient P-T, result in asymmetries of the 1.4 and 1.9-μm hydration bands, while the ammonium bands become clearly visible when the pressure drops below 10^{-2} mbar. Upon heating, the ammonium bands are almost stable below 523 K; the separation between the 2.02 and 2.13-μm absorptions tends to decrease at high-temperatures. The spectrum at 598 K is strongly affected by the thermal emission.

3.2.7. NH_4-Hectorite SHCa1

The spectra of NH_4-hectorite SHCa1 are shown in Figure 5 (right panels). According to chemical analyses reported in Che et al. (2011) this sample is substantially iron-free and Mg-rich, and also contains a small quantity of carbonate, as evidenced by a high calcium content (>13 wt%). Weak absorptions occurring at 0.96, 1.15, 1.4, and 2 μm are due to the hydration. The 1.4-μm band complex is composed of at least three different absorptions, located at 1.39, 1.41, and 1.46 μm. The 1.39-μm feature is due to OH, while the 1.41–1.46-μm are due to water

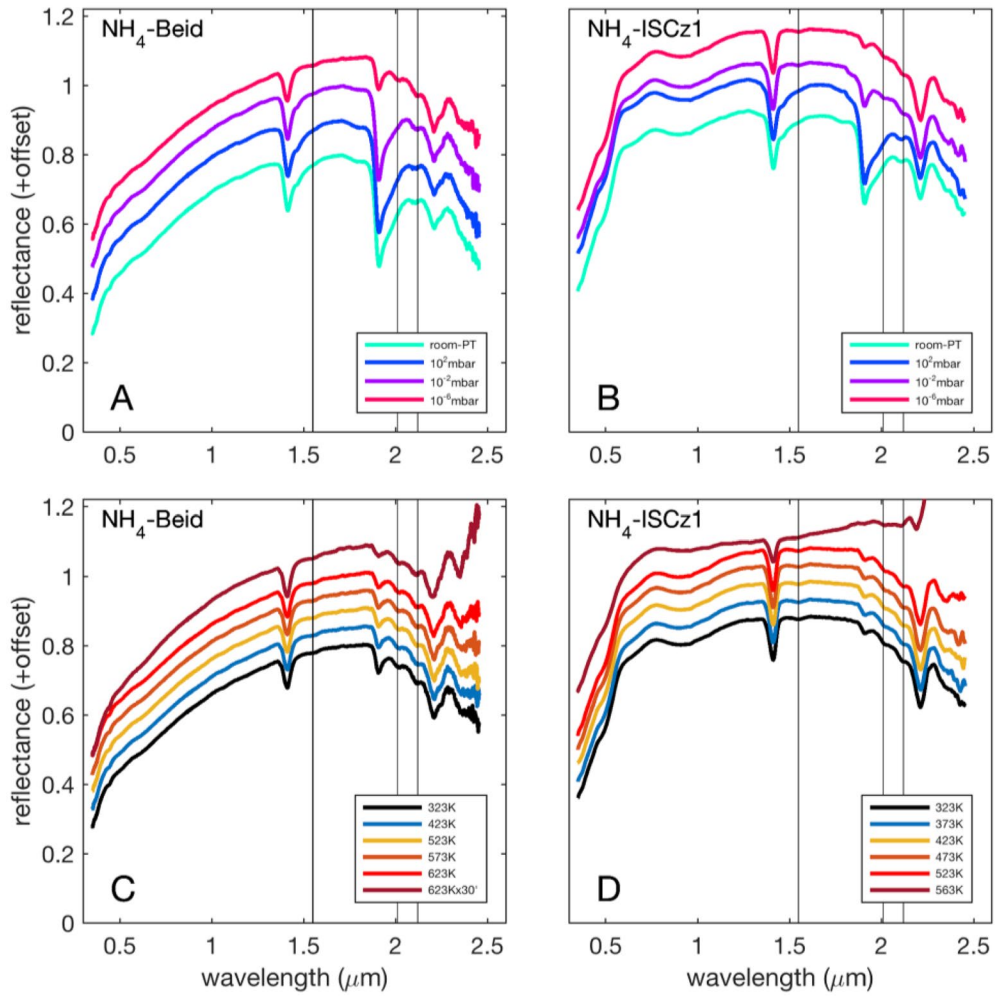

Figure 2. VNIR-Fieldspec spectra. The spectra above 2.4 μm are very noisy due to the small signal/noise of the setup in that spectral range. Top: spectra acquired at room T for decreasing pressures. Bottom: spectra acquired in vacuum at increasing temperatures. Vertical lines indicate the NH_4^+ absorptions.

molecules. The 2-μm complex is composed of two absorptions at 1.91 and 1.97 μm. The absorption at 2.31 μm is due to Mg-OH, while three weak absorptions that are located at 2.34, 2.39, and 2.43 μm, can be related to calcium carbonate in the sample. The NH_4^+ features are very weak and occur at 2.01 and 2.11 μm. The 1.55-μm ammonium band is extremely difficult to see in this sample. After pumping to high vacuum the water absorptions at 1.41 and 1.46 μm, as well as the 1.97 μm feature are removed, indicating these are related to weakly bound water. The two NH_4-bands are clearly visible in high vacuum below 10^{-3} mbar. These absorptions remain stable after heating below 523 K, while the high-T spectrum is affected by the thermal emission.

3.2.8. NH_4-Saponite SapBaj

Spectra of (natural) NH_4-SapBaj are displayed in Figure 6. This is an iron-rich saponite, as indicated by its visual reddish color and by Fe absorptions at 0.7–0.9 μm. Preliminary IR measurements indicated this sample was slightly naturally ammoniated. The room P-T spectrum is characterized by prominent hydration features at 1.4 and 1.9 μm, and by the Mg-OH band near 2.3 μm. As for the other samples, the only ammonium feature visible at room P-T condition is the one located near 2.12 μm. The other absorption band due to ammonium appears clear at 2.01 μm only after pumping in high vacuum and remains clear and separate while the temperature is increased. The 1.55-μm feature is almost not visible in this sample. For $T > 523$ K, the thermal emission begins to increase at wavelengths >2 μm, affecting the spectra at high-temperatures.

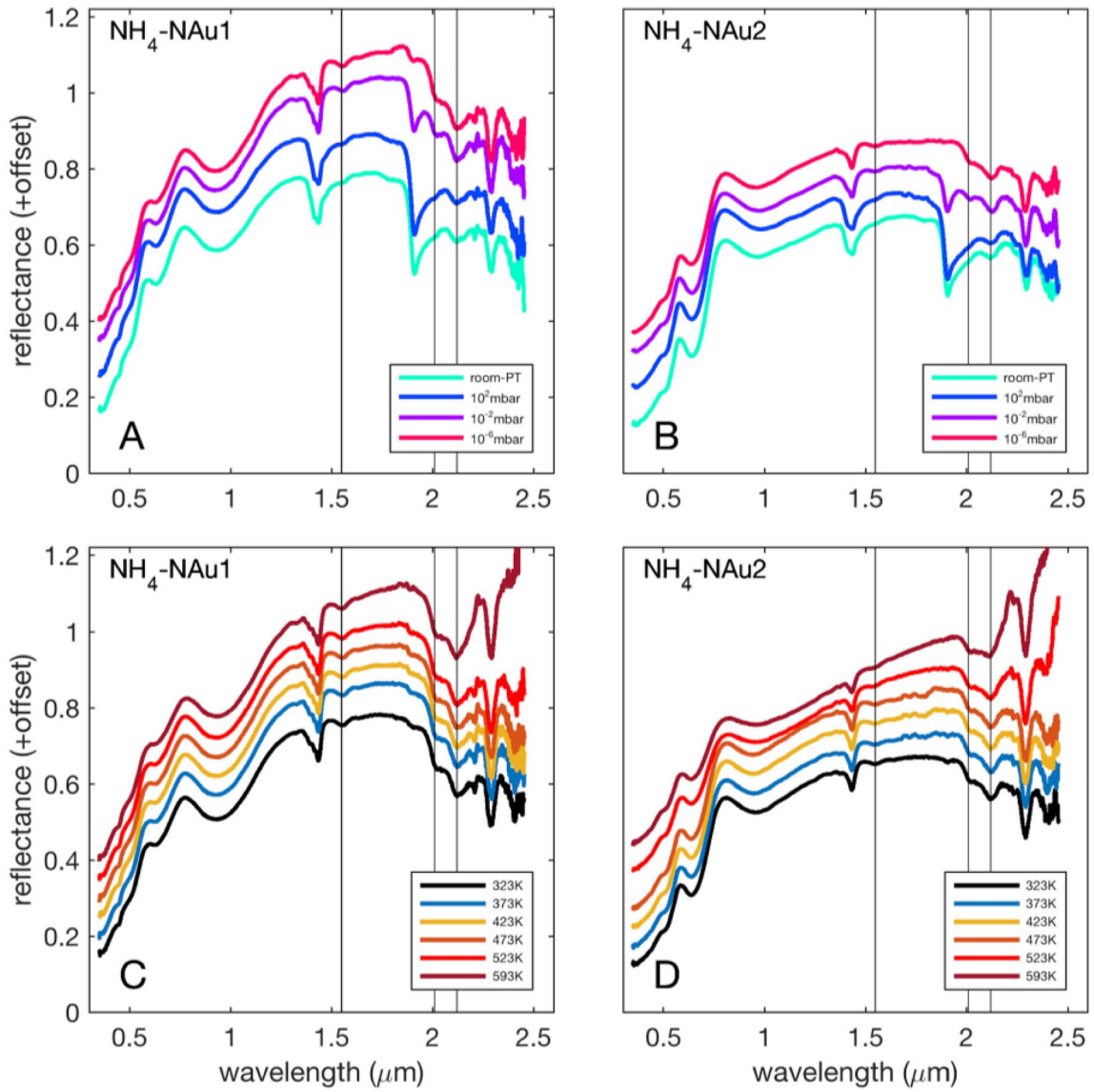

Figure 3. VNIR-Fieldspec spectra. The spectra above 2.4 μm are very noisy due to the small signal/noise of the setup in that spectral range. Top: spectra acquired at room T for decreasing pressures. Bottom: spectra acquired in vacuum at increasing temperatures. Vertical lines indicate the NH_4^+ absorptions.

3.3. IR: 1–5 μm

The spectra of phyllosilicates and NH_4-phyllosilicates acquired with SPIM in the IR region are displayed in Figures 7–10. It must be recalled that the samples have been heated in the oven for several days as described before. Data are shown in high vacuum (10^{-4}–10^{-5} mbar) and as a function of temperature. Room pressure/temperature spectra are shown for all samples for comparison (denoted as rPT). All spectra are generally characterized by (a) the fundamental OH stretching near 2.7 μm (Clark et al., 1990; Farmer, 1974), (b) the band due to adsorbed and interlayer water in the 2.9–3.2-μm region, (c) other superimposed features due to NH_4, and (d) eventually carbonates when present. Most of the samples have CaO content in the range 1–3 wt% except the hectorite sample SHCa1 with 14 wt% (Che et al., 2011), which contains nearly 50 wt% of carbonate (calcite + dolomite) (Chipera & Bish, 2001).

3.3.1. Beidellite Beid/NH_4-Beid

Spectra of beidellite and ammoniated beidellite are shown in Figures 7a and 7b. The broad and intense water absorption dominates the 3-μm region in the rPT spectrum (blue). The spectrum of beidellite (Figure 7a) is

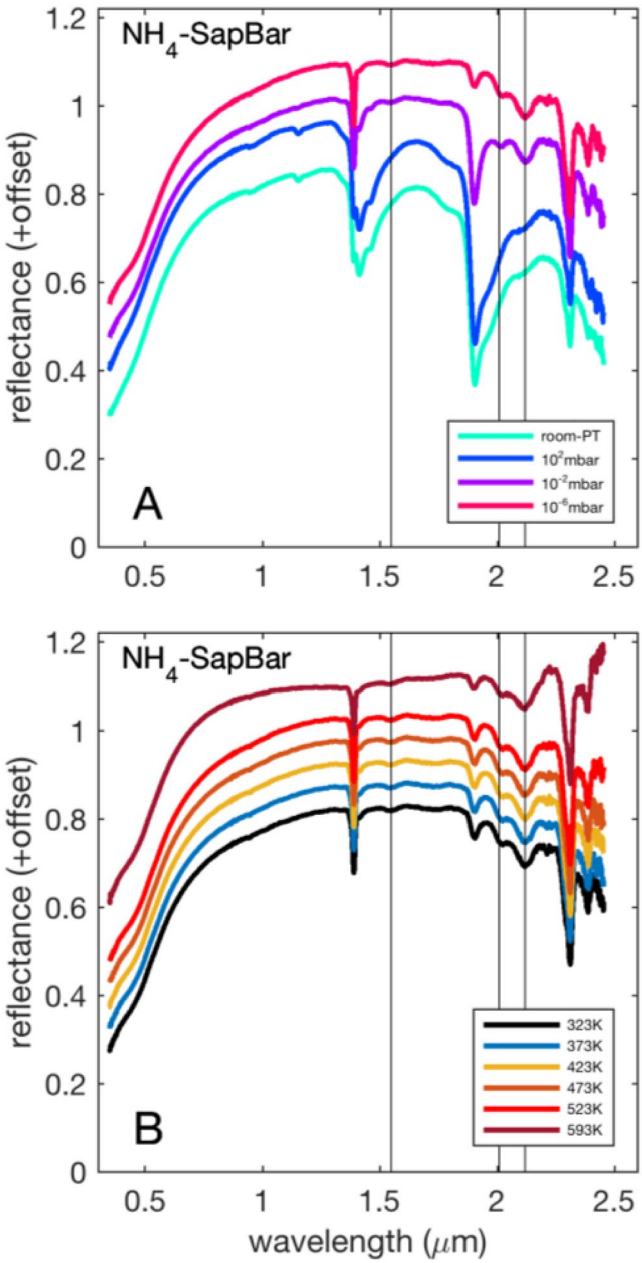

Figure 4. VNIR-Fieldspec spectra. The spectra above 2.4 μm are very noisy due to the small signal/noise of the setup in that spectral range. Top: spectra acquired at room T for decreasing pressures. Bottom: spectra acquired in vacuum for increasing temperatures. Vertical lines indicate the NH_4^+ absorptions.

characterized by absorption at 2.768 μm and absorption at 2.92 μm (Clark et al., 1990). The minimum at 2.76 μm is broad, indicating it consists of different overlapping absorptions due to OH. Due to different cation substitutions in this smectite, the crystalline order is reduced and the OH band is broad and consisting of two close absorptions, at 2.738 and 2.76 μm, with the short-wavelength one characteristic of beidellite and the long-wavelength one typical of montmorillonite domains; OH^- ions coordinated with various octahedral cations (Al^{3+}, Mg^{2+}, and Fe^{3+}) give different contributions (Farmer, 1974; Madejovà et al., 2017). In the spectrum (yellow) acquired at 423 K, the minimum near 2.74 μm is narrow and other relative minima appear at 3.01, 3.16, 3.34–3.45, and 3.98 μm. The features at 3.01 and 3.16 are related to water adsorbed/bound in the phyllosilicate. The other minima are likely due to the presence of some carbonate in the sample. At 523, 623, and 723 K the OH absorption is even narrower and located at 2.71 μm. The 3.01-μm water minimum is no longer visible while the 3.16-μm is still present. In the 723 K spectrum (green) most of the water is removed from the layers. The OH band remains, with the asymmetric V-shape likely due to residual water, and a weak absorption near 3.4 μm. In the rPT spectrum of the NH_4-beidellite (Figure 7b, blue) the OH stretch occurs at 2.768 μm; ammonium produces two bands: a V-shape band at 3.05 and a broad band centered at about 3.27 μm. In the 423 K spectrum (yellow) the OH band is narrower and located at 2.75 μm. The NH_4^+ features occur at 3.04 and as an inflection near 3.27 μm. Minima near 3.4–3.5 and 4 μm indicate the presence of carbonate in the sample. In the 523 K (red) and 623 K (purple) spectra, the OH band still appears at 2.75 μm, the ammonium features are at 3.04 (narrower) and near 3.27 μm. The minima due to carbonate appear more clearly. In the 723 K spectrum (green) the NH_4^+ feature at 3.04 μm has disappeared, and, in addition to the 2.7-μm OH band, only weak carbonate bands are visible in the 3.4–4 μm range.

3.3.2. Illite-Smectite ISCz1/NH_4-ISCz1

The spectra of ISCz1 are displayed in Figure 7c. In the pure not expandable illite a single narrow absorption is present in the OH-stretching region at 2.76 μm (Farmer, 1974; Madejovà et al., 2017). In our case, the sample is intermixed with smectite, thus the OH band is somewhat broader, although less than in the beidellite, and occurs at 2.75 μm in the rPT spectrum (blue). The intense absorption due to adsorbed water has a broad minimum near 2.95 μm and an inflection near 3.1 μm. In the 423 K spectrum (yellow) the OH minimum is shifted to 2.74 μm, the water contribution is greatly reduced, and it is possible to identify minima at 2.92, 3.02, and 3.16 μm due to H_2O molecules. Two features occurring at 3.38 and 3.98 μm could be related to the presence of carbonate in the sample. In the 523 and 623 K spectra the 3-μm water absorption is still split in minima at 2.9 and 3.01 μm. In the 723 K spectrum (green) the OH band at 2.7 μm is very narrow, with the asymmetry toward longer wavelengths indicating the presence of some residual water. The spectrum of the ammoniated-phase is displayed in Figure 7d. In the rPT spectrum (blue) the OH absorption occurs at 2.75 μm. The broad H_2O band has the minimum at 2.96 μm, an inflection near 3.1 μm (due to the absorption of NH_4^+) and relative minima at 3.38–3.5 due to carbonate. In the 423 K spectrum (yellow) the OH minimum is at 2.75 μm, and it is narrower. The ammonium band is separate and clearly visible at 3.05 μm. Two relative minima at 3.38–3.52 and 3.98 μm are due to carbonate. In the 523–623 K spectra (red/purple) the OH absorption is narrower and occurs at 2.75 μm. The

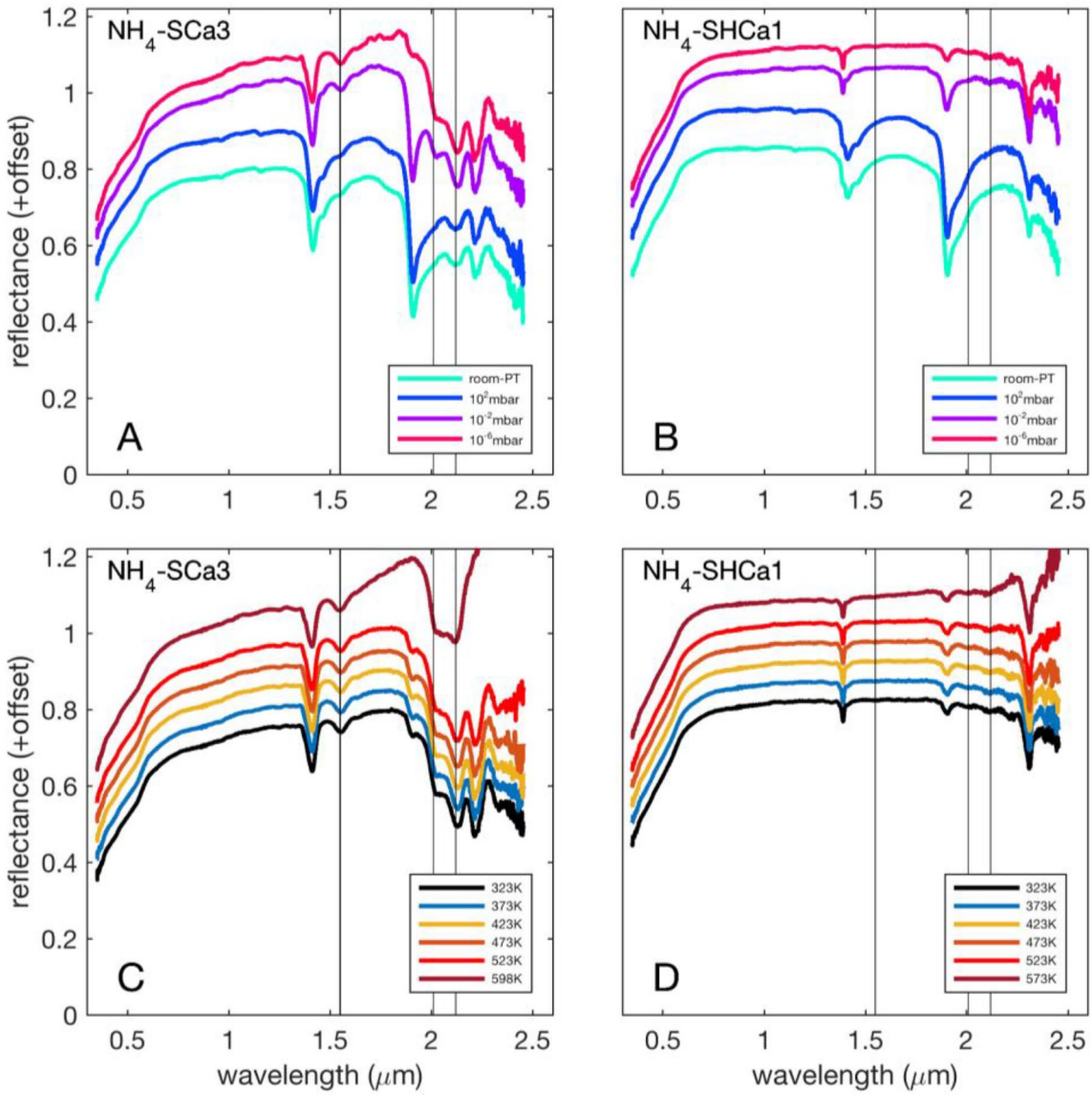

Figure 5. VNIR-Fieldspec spectra. The spectra above 2.4 μm are very noisy due to the small signal/noise of the setup in that spectral range. Top: spectra acquired at room T for decreasing pressures. Bottom: spectra acquired in vacuum for increasing temperatures. Vertical lines indicate the NH_4^+ absorptions.

NH_4^+ band minimum is at 3.05 μm. At 723 K (green spectrum) the ammonium band is no longer visible, although a shoulder near 3.1 μm can indicate the residual presence of some amount of ammonium.

3.3.3. Nontronite NAu1/NH_4-NAu1

The NAu1 spectra are shown in Figure 8a. In this type of smectites again the low crystalline order due to cation substitutions leads to broadening of OH absorptions; this feature is reported to occur at 3,563 cm^{-1} (2.81 μm) in transmission spectra, and is due to $Fe_2^{3+}OH$ or AlFeOH (Farmer, 1974; Frost & Kloprogge, 2000; Madejovà et al., 2017). In the rPT spectrum (blue) the OH absorption is located at 2.73 μm, the H_2O band is broad and with the minimum at 2.94 μm. In the 423, 523, and 623 K spectra (yellow, red, purple respectively) the water band is reduced, the OH absorption is more V-shaped, narrower and located at 2.73 μm. Secondary minima and inflections appear at 3.04, 3.16, related to interlayer water that is still present, and near 3.37 and 3.99 μm due to some carbonate. A weak feature also is visible at 3.62 μm. In the 623 K spectrum, the OH band at 2.7 μm is much narrower than at lower temperatures. In the 723 K spectrum, a slight broadening appears, maybe due to some loss of structural

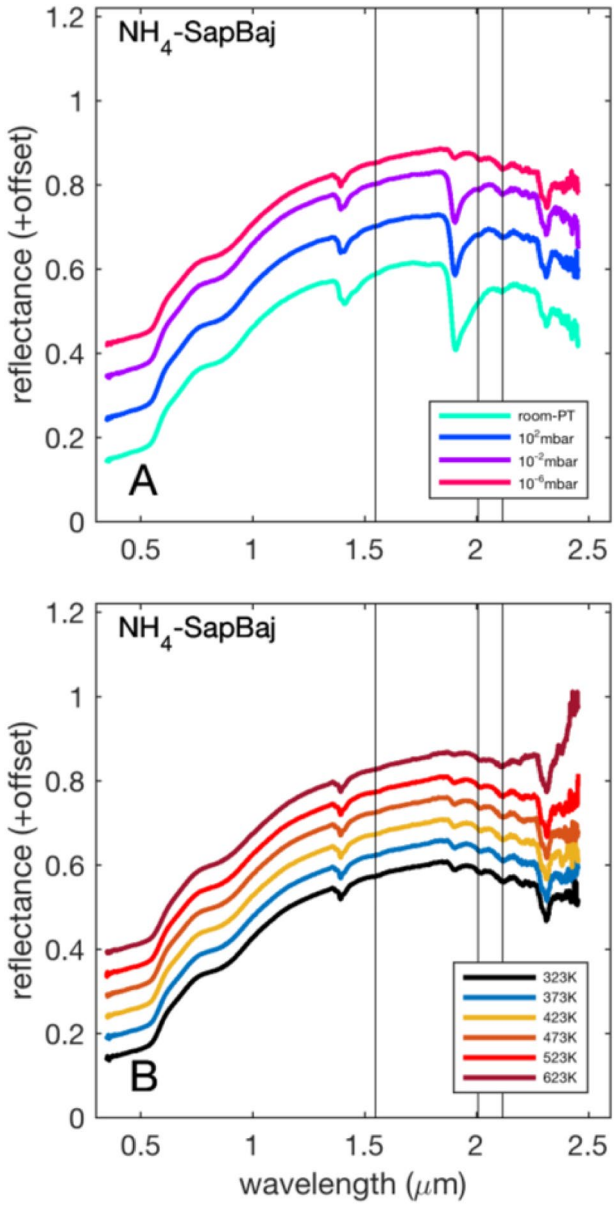

Figure 6. Spectra VNIR-Fieldspec. The spectra above 2.4 μm are very noisy due to the small signal/noise of the setup in that spectral range. Top: spectra acquired at room T during pressure decrease. Bottom: spectra acquired in vacuum during temperature rising. Vertical lines indicate the NH_4^+ absorptions.

order. In the NH_4-NAu1 rPT spectrum (Figure 8b, blue) the OH minimum is shifted and located at 2.79 μm, and the very large H_2O band is positioned at 3.02 μm. The water band complex is broader and shows additional relative minima and inflections at 3.1, 3.27 (H_2O, NH_4^+), 3.51 and 3.98 μm (CO_3^{2-}). In the 423 K spectrum (yellow) the OH feature is characterized by a minimum at 2.79 μm with an inflection shortward near 2.71 μm. The reduction of water allows recognizing the absorptions due to ammonium, located at 3.04 and 3.26 μm. The absorption near 3.5 μm is now clearly visible. In the 523 K spectrum, the absorptions due to OH (2.78 μm) and NH_4^+ (3.03 μm) become narrower and more separate. The 623 K spectrum is similar to the 523 K, with further narrowing of features. In the 723 K spectrum, no clear absorptions due to NH_4^+ appear, although the shoulder near 3.1 μm can indicate the presence of residual ammonium.

3.3.4. Nontronite NAu2/NH_4-NAu2

This sample is very similar in composition to the previous one, with only slightly less Al content and more Fe. The NAu2 rPT spectrum (Figure 8c, blue) is characterized by the OH absorption at 2.79 μm, consistent with the position of 3,573 cm^{-1} in transmission spectra (AlOH, Farmer, 1974; Madejovà et al., 2017; AlFeOH, Frost & Kloprogge, 2000). The water band complex is very large, with the minimum at 2.92 μm and actually masks every other spectral feature. The 423 K spectrum (yellow) water band is greatly reduced, the OH feature still occurs at 2.79 μm and secondary minima due mainly to interlayer water appear at 3.02–3.16 μm, while features at 3.37 and 3.98 μm indicate the presence of some minor amount of carbonate. In the 523–623 K spectra, the OH and H_2O absorptions occur at 2.79–3.02 μm, with the 3.16-μm feature becoming an inflection. In the NH_4-NAu2 rPT spectrum (Figure 8d, blue) the OH gives the absorption at 2.79 μm, with very poor separation from the very large H_2O band with a minimum near 3.02 μm. Weak inflections related to the CO_3^{2-} appear at 3.4–3.5 and 3.95 μm. In the 423, 523, and 623 K spectra the separation increases between OH (2.79 μm) and NH_4 (3.04 and 3.27 μm) features. The CO_3^{2-} absorptions are evident at 3.4–3.5 and 3.97–3.98 μm. The 723 K spectra of both ammoniated and non-ammoniated samples are very similar: in the latter, the ammonium band has disappeared as a separate feature. Both bands in the 2.7–3-μm region display a notable broadening, with the appearing of a second (OH or H_2O) band near 2.9 μm. The appearance of an OH doublet at 2.9 μm at high-temperatures is reported for Al-rich dioctahedral smectites (Farmer & Russell, 1967). Alternatively, this may be attributed to the appearance, once that most of the water has been removed, of the O-H stretching mode of the Fe-FeOH unit, which is reported to occur at 2.91–2.94 μm in ferruginous smectites and nontronites (Frost & Kloprogge, 2000).

3.3.5. Saponite SapBaj/NH_4-SapBaj

In the rPT spectrum of SapBaj (Figure 9a, blue) the OH feature has an inflection near 2.72 μm and the minimum at 2.78 μm. The hydroxyl absorption in this region is reported to occur at 2.69–2.72 μm due to Mg_3OH, and an additional band occurs at 2.76 μm in iron-rich saponite and griffithite (Farmer, 1974; Madejovà et al., 2017). Our sample is highly hydrated and also Fe-rich, thus the OH band is affected by such a crystalline environment. The water band is very broad and nearly flat, with a minimum at 2.91 μm. In the 423, 523, and 623 K spectra the absorptions due to OH and H_2O become clearly separate and distinct. The OH feature is shifted to 2.75 μm, while H_2O relative minima appear at 3.04 and 3.3 μm. Absorptions in the 3.3–3.5 μm and 3.98–4 μm regions could be again attributed to some carbonate. In the 723 K spectrum (green) most of the water has been removed

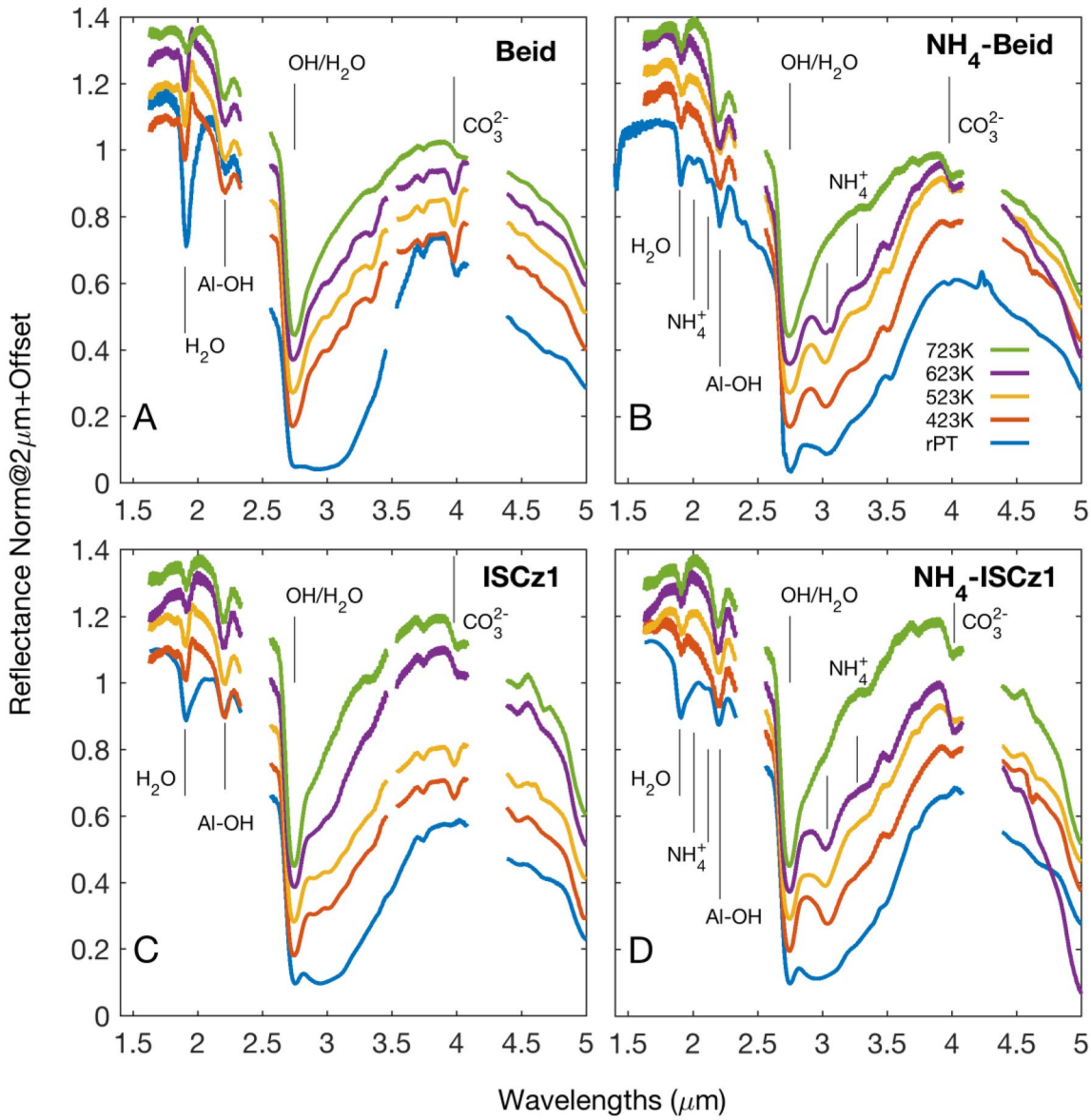

Figure 7. SPIM spectra of phyllosilicates/NH_4-phyllosilicates versus T (in vacuum). Samples have been heated at each temperature in the oven for a week, before measurements. The gap at 2.5-μm in SPIM spectra is due to instrument artifacts. The gap at 4.25 μm is due to the laboratory CO_2 absorption. NH_4-Beidellite at room PT: measured with FT-IR Bruker.

and many absorptions disappear. The OH feature is narrow and V-shaped, positioned at 2.74 μm, and weak bands remain at 3.35 and 4 μm. In the NH_4-SapBaj rPT spectrum (Figure 9b, blue) the OH is located at 2.76 μm and the whole 3-μm is broad, showing minima at 2.92 (H_2O) and 3.03 μm (H_2O + NH_4^+). A second inflection due to NH_4^+ occurs at 3.26 μm. In the 423 K (yellow) and 523 K (red) the OH absorption moves to 2.75 and 2.74 μm, the ammonium band occurs at 3.05 and 3.26 μm, and still appear weak CO_3^{2-} bands at 3.5 and 4 μm. The 723 K spectra of SapBaj and NH_4-SapBaj are very similar, with increasing narrowing, although a shoulder near 3.1 μm in the spectrum of the ammoniated sample could imply some NH_4^+ is still present.

3.3.6. Saponite SapBar/NH_4-SapBar

The iron content in this saponite is much less than in the previous sample, as indicated by VNIR spectra (Section 3.2). In the rPT spectrum of SapBar (Figure 9c, blue) the OH minimum is at 2.72 μm, additional H_2O minima/inflections are located at 2.76, 2.81, 2.92, and 3.07 μm. Two intense absorptions diagnostic of carbonate

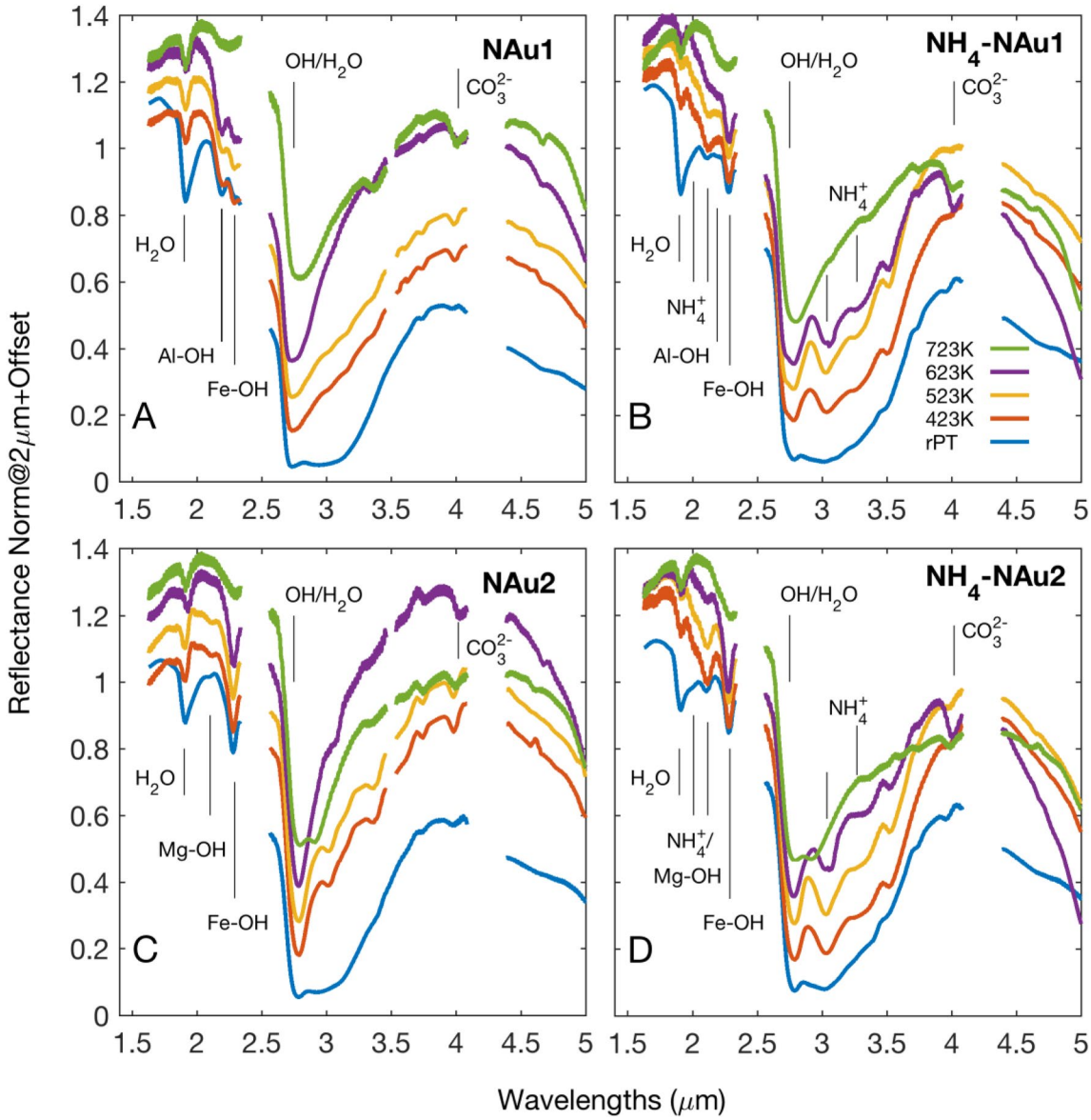

Figure 8. SPIM spectra of phyllosilicates/NH_4-phyllosilicates versus T (in vacuum). Samples have been heated at each temperature in the oven for a week, before measurements. The gap at 2.5-μm is due to instrument artifacts. The gap at 4.25 μm is due to the laboratory CO_2 absorption. Some instrument artifacts occurring at ~3.5 μm have been canceled.

occur at 3.4–3.5 and 3.8–4 μm. In the 423 K spectrum (yellow) the water content is still high; the OH produces an inflection at 2.73 μm and features due to H_2O appear at 2.85, 3.06 μm although still not separate. In the 523 K spectrum, the first H_2O minimum is shifted at 2.83 μm; the inflection at 3.06 μm is still visible. In the 623 K spectrum (purple) the water absorption above 3 μm, likely due to H_2O molecules linked to interlayer cations, appears clearly separate. The 723 K spectrum (green) is characterized by a clear V-shape narrow OH absorption at 2.72 μm, asymmetric toward longer wavelengths for some additional interlayer water (3.1 μm). The NH_4-Sap-Bar rPT spectrum is shown in Figure 9d (blue). The whole spectral region is dominated by intense water absorption. The OH is responsible for the sharp minimum at 2.72 μm, while H_2O produces features at 2.76, 2.92, and 3.07 μm. The intense water band masks the ammonium bands. In the 423 K (yellow) and 523 K (red) spectra the OH/H_2O minima are at 2.76–2.84 μm, while the 2.72-μm OH feature is only an inflection. The NH_4^+ band shows a clear absorption at 3.04 μm (as in the 623 K spectrum). The second ammonium band causes an inflection near 3.25 μm. The strong carbonate bands occur in all spectra at 3.4–3.5 and 4 μm. The 723 K spectrum displays a marked reduction of the H_2O band at 3 μm, while the ammonium absorption feature at 3.1 μm is still visible.

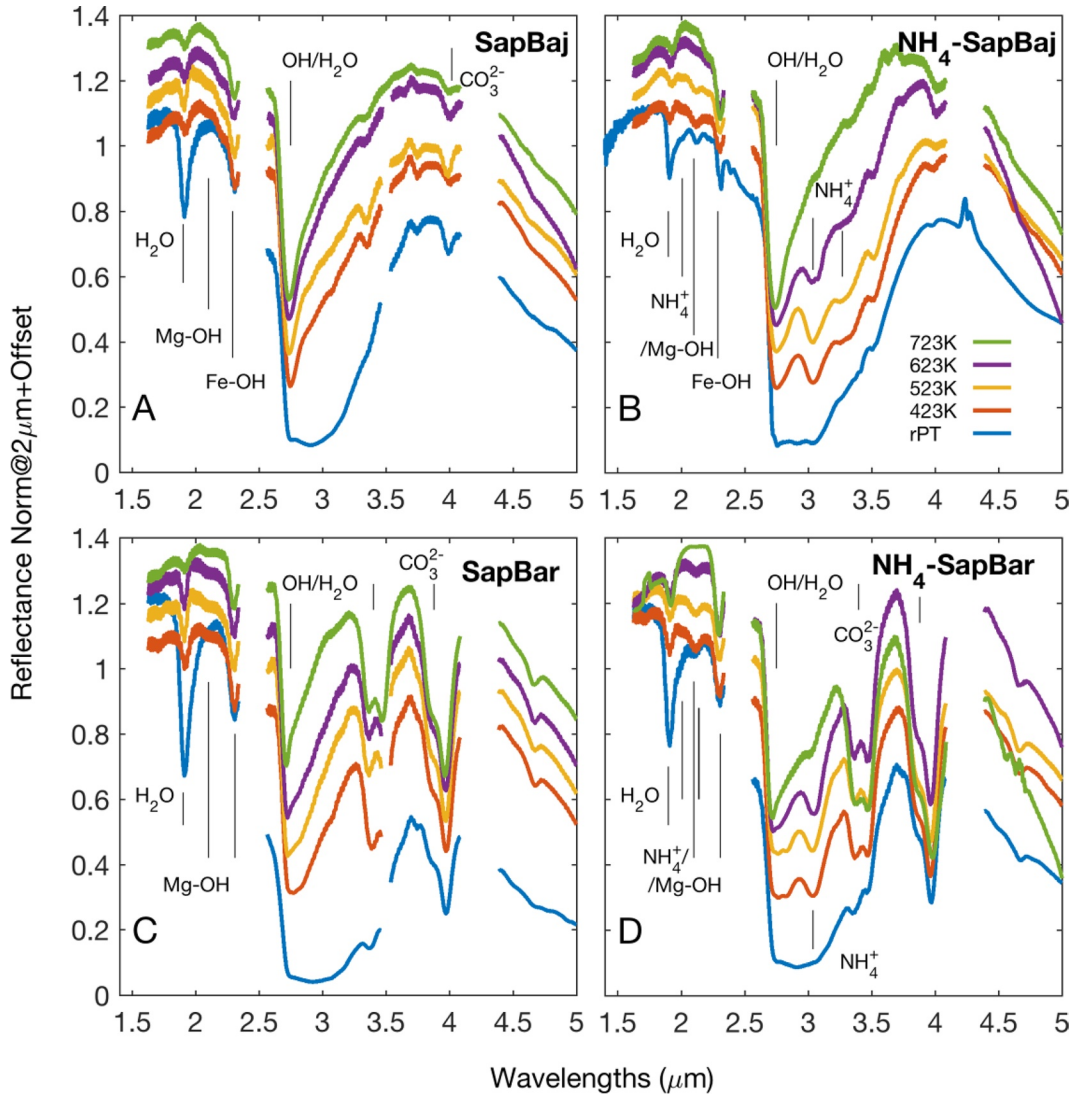

Figure 9. SPIM spectra of phyllosilicates/NH_4-phyllosilicates versus T (in vacuum). Samples have been heated at each temperature in the oven for a week, before measurements. The gap at 2.5-μm in SPIM spectra is due to instrument artifacts. The gap at 4.25 μm is due to the laboratory CO_2 absorption. NH_4-SapBaj at room PT: measured with FT-IR Bruker.

3.3.7. Montmorillonite SCa3/NH_4-SCa3

The rPT spectrum of SCa3 is shown in Figure 10a (blue). The OH stretching in montmorillonite occurs at longer wavelengths (2.78 μm) than in beidellite, occurring in octahedral sites (Farmer, 1974; Madejovà et al., 2017). The water absorption is very broad and strong, with a flat minimum around 3 μm. In the 423, 523, 623, and 723 K spectra the adsorbed/interlayer water is progressively removed: the band greatly reduces, it assumes a narrower V-shape and the OH absorption moves to 2.74 μm. Water produces inflections near 2.9 and 3.1 μm. The 3.1-μm feature gets more separate as the temperature increases then disappears at 723 K. Very weak features that remain at 3.38–3.5 and 4 μm indicate the presence of some carbonate in trace quantity. In Figure 10b (blue) the rPT spectrum of ammoniated SCa3 is displayed. It is still dominated by water in the sample, and relative minima are discernible at 2.75 μm (OH) and 3 μm (H_2O, broad). Ammonium bands, masked in the rPT spectrum, are clearly visible and well separate in the 423, 523, and 623 K spectra at 3.04–3.05 μm. With increasing temperature, the OH absorption band also gets narrower, well separate and moves toward 2.75 μm. The 723 K spectrum is V-shaped and with no NH_4^+ band appearing.

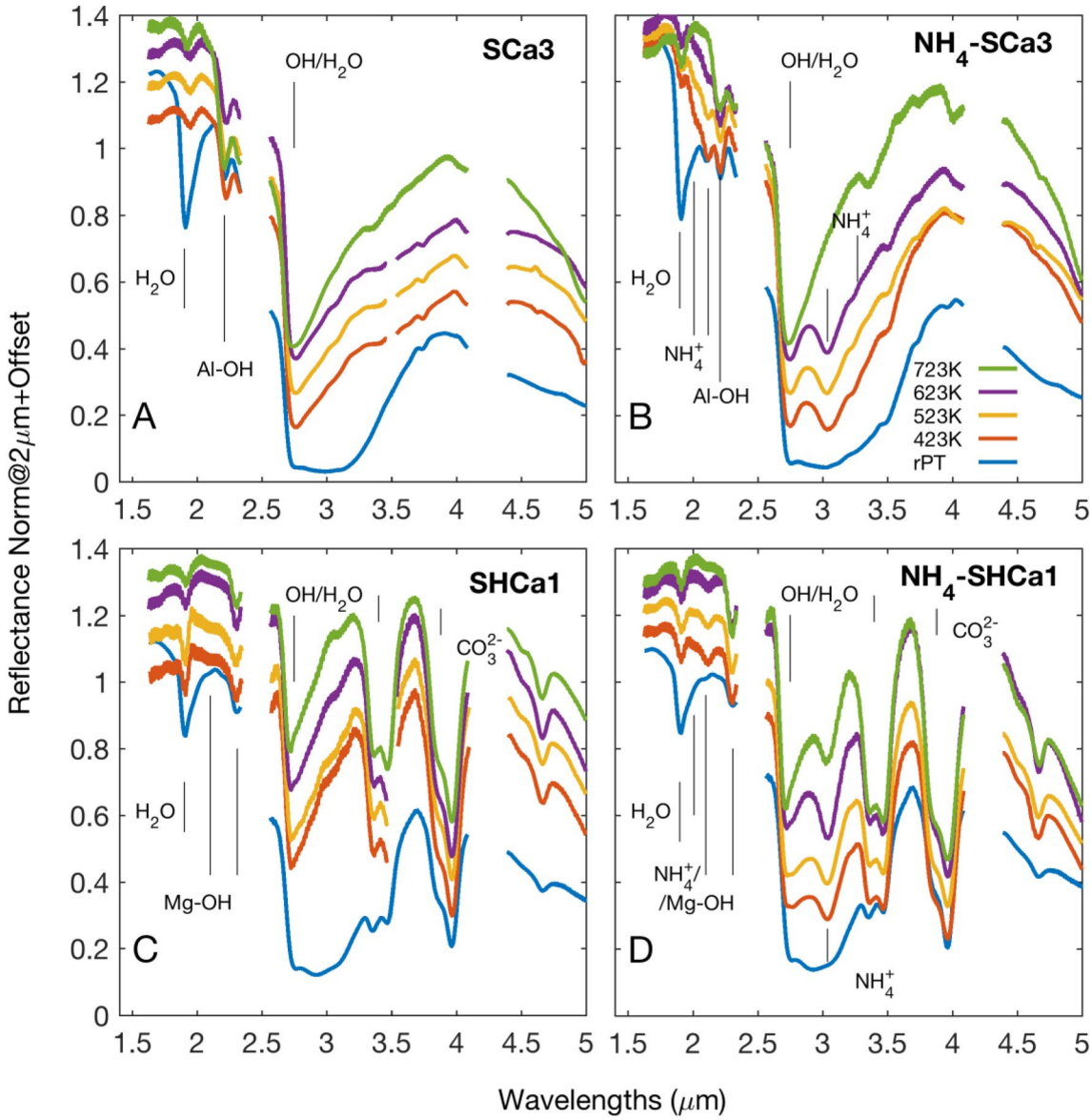

Figure 10. SPIM spectra of phyllosilicates/NH_4-phyllosilicates versus T (in vacuum). Samples have been heated at each temperature in the oven for a week, before measurements. The gap at 2.5-μm is due to instrument artifacts. The gap at 4.25 μm is due to the laboratory CO_2 absorption.

3.3.8. Hectorite SHCa1/NH_4-SHCa1

The OH stretching in hectorite occurs near 2.72 μm (3,680 cm^{-1}, $\nu(Mg_3OH)$), as reported in Farmer (1974) and Madejovà et al. (2017) for this sample, although in transmission spectra. In our rPT spectrum (Figure 10c) the 3-μm region is dominated by water, which affects the position of other features; the OH minimum here is located near 2.76 μm. Absorptions due to water appear at 2.92 and 3.12 μm. Strong carbonate bands occur at 3.4–3.5 and 4 μm. The 423–623 K spectrum is characterized by the OH absorption progressively at 2.74–2.72 μm and by H_2O features at 2.81 and at 3.04 μm. In the 723 K spectrum, the V-shaped OH absorption is narrow and located at 2.72 μm; some residual water firmly bound in the structure still affects the symmetry of the band and is responsible for the feature at 3.1 μm. The carbonate bands near 3.4 and 4 μm are still present. In the rPT spectrum of NH_4-SHCa1 (Figure 10d), the OH is responsible for the relative minimum at 2.76 μm, almost a shoulder of the intense water absorption positioned at 2.92 μm. The NH_4^+ bands appear well separate and clear in the 423 and 523K spectra, located at 3.04 μm. The secondary ammonium band occurs in high-temperature spectra near 3.24 μm. Two OH/H_2O minima occur at 2.73/2.77 μm in the high-T spectra, respectively, with the latter feature

reducing in intensity in the higher temperature spectrum. The two intense carbonate bands are present in all spectra. In the 723 K spectrum, the water absorption around 3 μm is greatly reduced although the 3.04 μm ammonium band is still well-separated and visible.

4. Discussion

Thanks to the pumping, heating and consequent dehydration, it has been possible to identify unambiguously the signatures of the ammonium in the infrared range. The ammonium in phyllosilicates creates several bands (Table 3) that can be used for the identification of such minerals on planetary surfaces. The ammonium band minima slightly shift for different phyllosilicates (see Table 3). In particular, the band at about 3.1 μm is the one that shows the largest variation. The NH_4^+ absorption at about 3.1 μm is due to the ν_3 stretching vibration (e.g., Petit et al., 1998; J. D. Russell 1965). The observed positions of the absorptions here reported are consistent with those for NH_4-bearing phases (Berg et al., 2016) and NH_4-smectites specifically (3.04–3.06 μm; Bishop, Banin, et al., 2002; Chourabi & Fripiat, 1981; Ehlmann et al., 2018; Ferrari et al., 2019; Petit et al., 1998). The position of the 3.1 μm (as well as of bands in the 1.5–2 μm region) relates to the kind of phyllosilicate hosting the ammonium. In this work, we focus our discussion on the 3-μm region in order to have a comparison with Ceres' data in the same spectral region, where the NH_4^+ band is observed. The quantitative analysis of the spectral parameters of all absorption bands (e.g., band position, depth, and FWHM) will be the subject of a follow-on study.

4.1. Ammonium Content Dependence on Temperature: Threshold Temperature

The spectra here reported clearly show the signatures of the ammonium cation in the phyllosilicate. Qualitatively the ammonium content, as visible in the 3-μm region in SPIM spectra (Figures 7–10), is progressively reduced as the temperature is raised. The band depth decreases at higher temperatures, as can be seen qualitatively by looking at the 3.1/2.7-μm minimum ratio. In the <523 K-spectra of all samples the 3.1/2.7-μm minimum ratio is around 1, maybe indicating a roughly equal presence of OH/NH_4 in the samples. In the 723 K spectra the ammonium band at 3.1 μm is no longer visible as a separate feature, except than in NH_4-ISCz1 (as shoulder), NH_4-SapBar and NH_4-SHCa1, in which this band still remains well visible. Thus in the 723 K-spectra of these three samples, the ratio is about 0.5, indicating the ammonium content still could be 50% of the initial value. In the other samples, the ammonium band is no longer visible in the 723 K-spectra, although the asymmetry of the 3-μm feature can indicate that some ammonium may still be present, likely a small fraction of the initial content.

4.2. 3.1-μm Band: H_2O Versus NH_4^+

The spectral region around 3 μm in water-bearing minerals is very difficult to analyze. Indeed, the absorption feature at about 3.1-μm is present in the ammoniated samples and in several non-ammoniated samples (even if the features are quite different). At this wavelength, both NH_4^+ and H_2O absorptions can occur and overlap. The ammonium feature at about 3.1-μm is due to the fundamental stretching vibration in NH_4^+. Water is responsible for two absorptions at this wavelength, the symmetric stretching (3,220 cm^{-1}/3.1 μm) plus an overtone at 3,240–3,250 cm^{-1} (3.08 μm) of the fundamental bending (1,630 cm^{-1}/6 μm) (Farmer, 1974; Farmer & Russell, 1967). The water band at 3.1 μm in minerals/rocks has been described by several authors (Aines & Rossman, 1984; Farmer, 1974; Farmer & Russell, 1967; Fukuda, 2012; Johnston, 2017). Farmer and Russell (1967) describe as in Mg-saponite this band is clearly visible and intense upon dehydration, at least up to 200°C. This feature is attributed to H_2O molecules that are attached directly to interlayer cations, after that the outer spheres of hydration have been removed (by dehydration or evacuation) so that strong ion-dipole interactions between Mg^{2+} and H_2O molecules can form (Johnston, 2017). In Mg-hectorite water molecules attached to interlayer cations form H-bonds with water of outer spheres of hydration, giving a band near 3.09 μm (Farmer & Russell, 1967). In general, such bands appearing beyond 3,300 cm^{-1} ($\lambda > 3.03$ μm) are indicative of strong hydrogen bonds. Thus, it is difficult to distinguish between the signature of NH_4^+ and H_2O when the samples are rich in water. However, the distinction is easier when the samples dehydrate, as we have reported here.

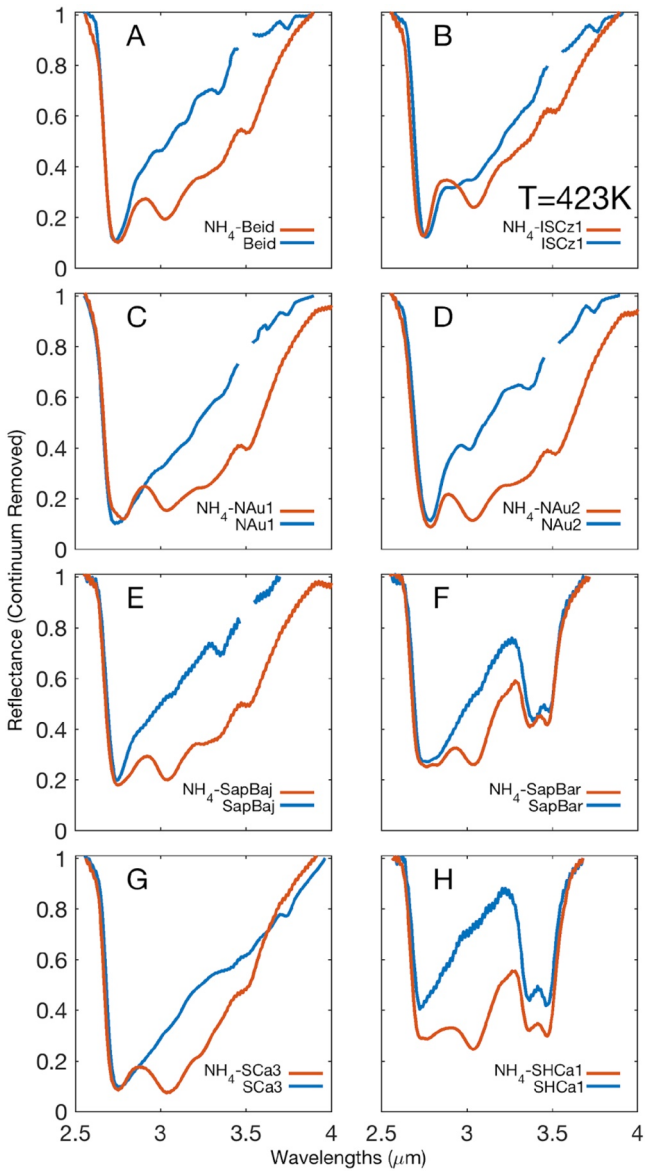

Figure 11. IR spectra of phyllosilicates and NH_4-phyllosilicates: continuum removed 3-μm band. Comparison at $T = 423$ K.

4.3. Dehydration of Phyllosilicates Versus NH_4^+-Phyllosilicates

When the samples are heated for several days at different temperatures, the 3-μm band in the ammoniated and non-ammoniated samples starts to be different. Comparing spectra of dehydrated phyllosilicates and corresponding NH_4-phyllosilicates at the same temperature (423 K, Figure 11) it appears that the 3-μm band in ammoniated samples is generally broader and considerably more intense than in the corresponding non-ammoniated samples. This can be an indication that dehydration occurs much more slowly in ammoniated samples. Such behavior could be explained with the observation that in presence of polar interlayer cations (i.e., NH_4^+) in phyllosilicates, water molecules that are attached to interlayer cations develop more intense hydrogen bonds with water in outer spheres of coordination (Farmer & Russell, 1967; Russell & White, 1966). It must be noted that both phyllosilicates and NH_4-phyllosilicates are readily "saturated" in water content when exposed to ambient air with typical humidity. When the sample is maintained in the oven at higher temperatures, the spectra of the non-ammoniated samples do not show anymore a clear 3-μm band, while the ammoniated ones have a clear V-shape band in the 3 μm region. With the temperature increase, the overall spectra changes: the proportion between the band strength of the 2.7 and 3-μm signature changes, with a reduction of the 3-μm and a narrowing of the 2.7-μm.

4.4. Comparison With Ceres Spectra

Ceres is an airless body and its surface is almost in vacuum. Thus, it is reasonable to compare Ceres spectra (Raponi et al., 2019) with the spectra of dehydrated phyllosilicates, both ammoniated and not. In particular, we compare the high-temperature spectra of NH_4-phyllosilicates, showing the largest dehydration, with the average spectrum of Ceres as measured by VIR (Figure 12). VIR data show a clear narrow band at 2.72–2.73 μm and a band at about 3.1 μm, whose shapes are not fully compatible with spectra of ammoniated samples at ambient T-P here reported, as well as the spectra reported in previous articles (Berg et al., 2016; Bishop, Banin, et al., 2002; Ehlmann et al., 2018; Ferrari et al., 2019). Ceres average spectrum has been interpreted as the result of a mixture of Mg-phyllosilicate, ammoniated phyllosilicate, carbonate and a large amount of a dark opaque phase, likely carbon or magnetite (De Sanctis, Ammannito, et al., 2015; Marchi et al., 2019; Raponi et al., 2019). Here we compare the spectrum of Ceres, which is a mixture of different minerals, with the measured spectra of the ammoniated phyllosilicates, recalling that the ammoniated-phase is only one of the components of the mixture. Thus, the comparison we are reporting here is only qualitative and can give insight into the most likely carrier of the ammonium on Ceres. We compare the laboratory spectra of the ammoniated-phase and non-ammoniated-phase at the highest temperature (723 K) and the spectra of the ammoniated-phase taken at a 100 K lower temperature (623 K) (Figure 12). We limit our comparison to the band at 2.73 and 3.1 μm. The laboratory spectra at 723 K almost do not show any signature at 3.1 μm (except that for NH_4-SapBar and NH_4-SHCa1), that indeed strongly characterize the Ceres spectrum, while the spectra of the ammoniated samples at 623 K still show such band.

The shape of the 3.1 μm band of the laboratory samples compared with the Ceres' corresponding band is very similar. The other interesting and characteristic feature is the band at 2.72–2.73 μm. This band is likely due to Mg-OH. The Ceres 2.72–2.73 μm band is very narrow and only a few of the samples measured here show a similar band. In Table 3 the minima of 2.7-μm (OH) and 3.1-μm (NH_4^+) absorption bands of NH_4-phyllosilicates retrieved at 623 K are listed. This temperature has been chosen as the higher one still showing the ammonium feature, but

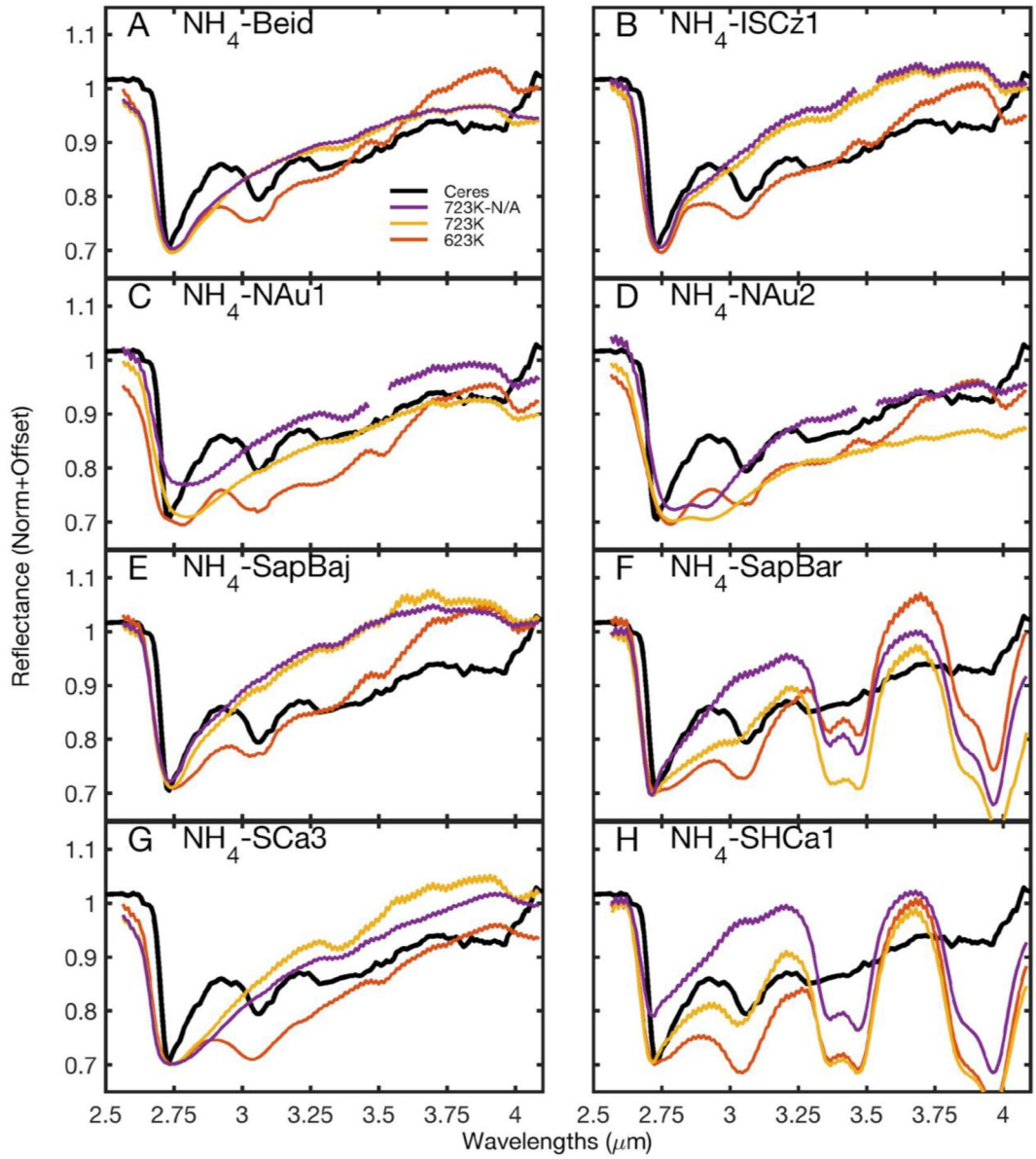

Figure 12. Ceres-VIR spectrum (Raponi et al., 2019) compared with NH_4-Phyllosilicates at two different temperatures (623−723 K). For each NH_4-phyllosilicate also the spectrum of the corresponding non-ammoniated sample at 723 K is shown.

trying to remove the water in excess. These positions are compared with the 2.72 and 3.06 μm positions (minima) of corresponding bands in the average spectrum of Ceres, as measured by VIR. Putting together the shapes of the 2.72–2.73 and 3.1 μm bands, we see that the ammoniated phyllosilicates that most resemble the Ceres spectrum are NH_4-SapBar and NH_4-SHCa1. In fact, although four samples show a similar position (3.05 μm) for the ammonium feature, that is the two NH_4-nontronites, NH_4-SapBar and NH_4-SHCa1, only the two latters also display a similar position of the OH band (2.72 μm). Anyway, if we do not consider the ammonium feature at 3.1 μm, thus hypothetically we only compare the OH band shape independently from the presence of ammonium, the V-shape of the OH absorption at 2.7 μm is best matched by the 723 K spectra of NH_4-ISCz1 and NH_4-SapBaj, although the minimum position is slightly shifted with respect to Ceres. The remaining samples show appreciable differences in terms of the 2.7 band center and shape. The NH_4-SapBar and NH_4-SHCa1 samples are indeed Mg-rich phyllosilicates, while the others are Fe-rich (nontronites and saponite SapBaj) or Al-rich phyllosilicates (montmorillonite, beidellite), thus characterized by the OH absorption more shifted toward longer wavelengths (2.75–2.80 μm). The measurements

Table 4
Wavelength Locations of the Minima of 2.7 (OH^-) and 1.55, 2.01, 2.12, and 3.1-μm (NH_4^+) Bands in Spectra of NH_4-Phyllosilicates, at 623 K

Sample	1.55-μm	2.02-μm	2.12-μm	2.7-μm	3.1-μm
NH_4-beid	1.55	2.01	2.12	2.75	3.03
NH_4-ISCz1	1.55	2.02	2.11	2.75	3.03
NH_4-NAu1	1.56	2.02	2.12	2.79	3.05
NH_4-NAu2	1.55	2.01	2.12	2.78	3.05
NH_4-SapBaj	–	2.02	2.12	2.75	3.03
NH_4-SapBar	1.55	2.02	2.12	2.72	3.05
NH_4-SCa3	1.55	2.02	2.13	2.75	3.04
NH_4-SHCa1	–	2.01	2.11	2.72	3.05

Note. In Ceres' average spectrum, minima are at 2.72μm and 3.064 μm respectively.

here reported corroborate the identification of NH_4-phyllosilicate on Ceres, in particular Mg-rich NH_4-smectite. The average Ceres spectrum is compatible with the presence of dehydrated ($T > 623$ K) Mg-phyllosilicate with the best match being NH_4-SapBar and NH_4-SHCa1. These measurements can help in refining our knowledge of Ceres surface composition and to constrain the evolution of this dwarf planet (Table 4).

5. Conclusions

Reflectance spectra of phyllosilicates and NH_4-phyllosilicates have been investigated in the VIS-IR range at different pressure-temperature conditions, both at ambient P-T and in high vacuum/high-T conditions. Spectral changes in band positions and shapes occur in vacuum and as the temperature rises, as long as the adsorbed and interlayer water is removed from samples. In particular, in the IR range the NH_4^+ bands at 1.55, 2.01, 2.12, and 3.1 μm become clearly separate and discernible as the samples are first pumped down and then dehydrated and the masking water absorptions are reduced. In the 2-μm region, the high vacuum is sufficient to remove nearly completely the hydration band. High-temperature spectra of ammonium phyllosilicates in the 3-μm region are characterized by the increasing separation and narrowing of OH^- (2.7 μm) and NH_4^+ (3.1 μm) absorption bands. The exact position of the 3.1-μm band varies in the 3.03–3.1 μm range depending on the phyllosilicate, due to the particular lattice and interlayer cations characterizing the mineral structure. A very small absorption feature occurring near 3.1 μm in high-temperature spectra of some non-ammoniated samples (saponite and hectorite) must be ascribed to water coordinated directly to interlayer cations. The spectra of non-ammoniated samples and corresponding NH_4-phyllosilicates acquired at a given (same) high-temperature are quite different: spectra of NH_4-phyllosilicates show the 3-μm band complex considerably broader and more intense than occurs for non-ammoniated samples. Thus in order to obtain spectra of NH_4-samples with a very narrow and V-shaped OH stretching absorption band, higher temperatures must be reached. This observation can have implications for the interpretation of remote-sensing spectra of asteroids. From a comparison of high-temperature spectra of NH_4-phyllosilicates with Ceres average spectrum measured by VIR it results that the best match in terms of spectral shape and OH/NH_4^+ position occurs for Mg-rich phyllosilicates, in particular, NH_4-saponite and NH_4-hectorite.

Data Availability Statement

The complete sets of data (De Angelis, Ferrari, De Sanctis, Ammannito, et al., 2020) presented in this study are available online upon publication of this study in the INAF Repository (https://vwww.ict.inaf.it): https://doi.org/10.20371/INAF/DS/2020_00002. For the Ceres spectrum data shown in Figure 12 please refer to Raponi et al. (2019).

Acknowledgments
Ambient P-T spectra of NH_4-Beidellite and NH_4-SapBaj were acquired, in the 3-μm range, by means of the FTIR spectrometer in P-LAB at IAPS; the authors are very grateful to Dr. Stefania Stefani and Dr. Giuseppe Piccioni (INAF-IAPS, Rome, Italy). The authors also are very grateful to Dr. Giovanna Agrosì and Dr. Gioacchino Tempesta (University of Bari, Italy) for XRPD analyses of samples. The authors wish to thank ASI for funding our project with Grant ASI I/004/12/2 and with ExoMars program. Open Access Funding provided by Istituto nazionale di astrofisica.

References

Aines, R. D., & Rossman, G. R. (1984). Water in minerals? A peak in the infrared. *Journal of Geophysical Research*, *89*(B6), 4059–4071. https://doi.org/10.1029/jb089ib06p04059

Ammannito, E., De Sanctis, M. C., Ciarniello, M., Frigeri, A., Carrozzo, F. G., Combe, J.-Ph., et al. (2016). Distribution of phyllosilicates on the surface of Ceres. *Science*, *353*(6303), aaf4279. https://doi.org/10.1126/science.aaf4279

Berg, B. L., Cloutis, E. A., Beck, P., Vernazza, P., Bishop, J. L., Takir, D., et al. (2016). Reflectance spectroscopy (0.35–8μm) of ammonium-bearing minerals and qualitative comparison to Ceres-like asteroids. *Icarus*, *265*, 218–237. https://doi.org/10.1016/j.icarus.2015.10.028

Bishop, J. L., Banin, A., Mancinelli, R. L., & Klovstad, M. R. (2002). Detection of soluble and fixed NH_4^+ in clay minerals by DTA and IR reflectance spectroscopy: A potential tool for planetary surface exploration. *Planetary and Space Science*, *50*(1), 11–19. https://doi.org/10.1016/s0032-0633(01)00077-0

Bishop, J. L., & Pieters, C. M. (1995). Low-temperature and low atmospheric pressure infrared reflectance spectroscopy of Mars soil analog materials. *Journal of Geophysical Research*, *100*(E3), 5369–5379. https://doi.org/10.1029/94je03331

Bishop, J. L., Pieters, C. M., & Edwards, J. O. (1994). Infrared spectroscopic analyses on the nature of water in montmorillonite. *Clays and Clay Minerals*, *42*(6), 702–716. https://doi.org/10.1346/ccmn.1994.0420606

Blake, R. L. (1965). Iron phyllosilicate of the Cuyuna district in Minnesota. *American Mineralogist*, *50*(1–2), 148–169.

Bruno, T. J., & Svoronos, P. D. N. (1989). *Handbook of basic tables for chemical analysis*. CRC Press.

Che, C., Glotch, T. D., Bish, D. L., Michalski, J. R., & Xu, W. (2011). Spectroscopic study of the dehydration and/or dehydroxylation of phyllosilicate and zeolite minerals. *Journal of Geophysical Research*, *116*(E5), E05007. https://doi.org/10.1029/2010JE003740

Chipera, S. J., & Bish, D. L. (2001). Baseline studies of the clay minerals society source clays: Powder X-Ray diffraction analyses. *Clays and Clay Minerals*, *49*(5), 398–409. https://doi.org/10.1346/ccmn.2001.0490507

Chourabi, B., & Fripiat, J. J. (1981). Determination of tetrahedral substitutions and interlayer surface heterogeneity from vibrational spectra of ammonium in smectites. *Clays and Clay Minerals*, *29*(4), 260–268. https://doi.org/10.1346/ccmn.1981.0290403

Clark, R. N., King, T. V. V., Klejwa, M., Swayze, G., & Vergo, N. (1990). High spectral resolution reflectance spectroscopy of minerals. *Journal of Geophysical Research*, *95*(B8), 12653–12680. https://doi.org/10.1029/jb095ib08p12653

Coradini, A., Ammannito, E., Boccaccini, A., Di Iorio, T., Baldetti, P., Capaccioni, F., et al. (2011). Laboratory measurements in support of the DAWN mission: The SPectral IMaging (SPIM) facility. In *EPSC Abstracts, EPSC-DPS2011-1043, EPSC-DPS Joint Meeting* (Vol. 6).

De Angelis, S., Ammannito, E., Di Iorio, T., De Sanctis, M. C., Manzari, P. O., Liberati, F., et al. (2015). The spectral imaging facility: Setup characterization. *Review of Scientific Instruments*, *86*(9), 093101. https://doi.org/10.1063/1.4929433

De Angelis, S., Ferrari, M., De Sanctis, M. C., Ammannito, E., Raponi, A., & Ciarniello, M. (2020). *High-vacuum/high-temperature reflectance Spectroscopy of Phyllosilicates and NH4-Phyllosilicates in the visible-near infrared range*. INAF-ICT Repository. https://doi.org/10.20371/INAF/DS/2020_00002

De Angelis, S., Ferrari, M., De Sanctis, M. C., Biondi, D., Boccaccini, A., Morbidini, A., et al. (2018). Design, development and testing of an environmental P-T cell for InfraRed spectroscopy measurements. *Review of Scientific Instruments*, *89*(10), 103107. https://doi.org/10.1063/1.5047038

De Angelis, S., Manzari, P., De Sanctis, M. C., Altieri, F., Carli, C., & Agrosì, G. (2017). Application of spectral linear mixing to rock slabs analyses at various scales using Ma_Miss BreadBoard instrument. *Planetary and Space Science*, *144*, 1–15. https://doi.org/10.1016/j.pss.2017.06.005

De Sanctis, M. C., Ammannito, E., Raponi, A., Marchi, S., McCord, T. B., McSween, H. Y., et al. (2015). Ammoniated phyllosilicates with a likely outer Solar System origin on (1) Ceres. *Nature*, *528*(7581), 241–244. https://doi.org/10.1038/nature16172

De Sanctis, M. C., Coradini, A., Ammannito, E., Filacchione, G., Capria, M. T., Fonte, S., et al. (2011). The VIR spectrometer. *Space Science Reviews*, *163*, 329–369. https://doi.org/10.1007/s11214-010-9668-5

Diaz Pinthier, M. (1999). *Étude des interactions cations compensateurs/feuillets dans les argiles: Contribution à la connaissance des mécanismes de rétention sélective* (Ph. D. Thesis). Orléans University.

Earnest, C. M. (1983a). Thermal analysis of hectorite. Part I. Thermogravimetry. *Thermochimica Acta*, *63*(3), 277–289. https://doi.org/10.1016/0040-6031(83)80325-6

Earnest, C. M. (1983b). Thermal analysis of hectorite. Part II. Differential thermal analysis. *Thermochimica Acta*, *63*(3), 291–306. https://doi.org/10.1016/0040-6031(83)80326-8

Ehlmann, B. L., Hodyss, R., Bristow, T. F., Rossman, G. R., Ammannito, E., De Sanctis, M. C., & Raymond, C. A. (2018). Ambient and cold-temperature infrared spectra and XRD patterns of ammoniated phyllosilicates and carbonaceous chondrite meteorites relevant to Ceres and other solar system bodies. *Meteoritics & Planetary Science*, *53*(9), 1884–1901. https://doi.org/10.1111/maps.13103

Farmer, V. C. (Ed.). (1974). *The infrared spectra of minerals*. Mineralogical Society. https://doi.org/10.21236/ad0781679

Farmer, V. C., & Russell, J. D. (1967). Infrared absorption spectrometry in clay studies. *Fifteenth Conference on Clays and Clay Minerals*.

Ferrari, M., De Angelis, S., De Sanctis, M. C., Ammannito, E., Stefani, S., & Piccioni, G. (2019). Reflectance spectroscopy of ammonium-bearing phyllosilicates. *Icarus*, *321*, 522–530. https://doi.org/10.1016/j.icarus.2018.11.031

Formisano, M., De Sanctis, M. C., Capria, M. T., Ammannito, E., Capaccioni, F., Magni, G., et al. (2015). Water sublimation and surface temperature simulations of Ceres. In *46th Lunar and Planetary Science Conference, abstract #2405*.

Frost, R. L., & Kloprogge, J. T. (2000). Vibrational spectroscopy of ferruginous smectite and nontronite. *Spectrochimica Acta: Part A*, *56*(11), 2177–2189. https://doi.org/10.1016/s1386-1425(00)00279-1

Fukuda, J. I. (2012). Water in rocks and minerals – Species, distributions, and temperature dependences. In T. Theophanides (Ed.), *Infrared Spectroscopy, Materials Science, Engineering and Technology*. https://doi.org/10.5772/2055

Gailhanou, H., Van Miltenburg, J. C., Rogez, J., Olives, J., Amouric, M., Gaucher, E. C., & Blanc, P. et al. (2007). Thermodynamic properties of anhydrous smectite MX-80, illite IMt-2 and mixed-layer illite–smectite ISCz-1 as determined by calorimetric methods. Part I: Heat capacities, heat contents and entropies. *Geochimica et Cosmochimica Acta*, *71*(22), 5463–5473. https://doi.org/10.1016/j.gca.2007.09.020

Johnston, C. T. (2017). Infrared studies of clay mineral-water interactions. In W. P. Gates, J. T. Kloprogge, J. Madejová, F. Bergaya (Eds.), *Infrared and Raman spectroscopies of clay minerals* (Vol. 8, pp. 1–604).

King, T. V. V., Clark, R. N., Calvin, W. M., Sherman, D. M., & Brown, R. H. (1992). Evidence for ammonium-bearing minerals on Ceres. *Science*, *255*(5051), 1551–1553. https://doi.org/10.1126/science.255.5051.1551

Knop, O., Oxton, I. A., & Falk, M. (1979). Infrared spectra of the ammonium ion in crystals. Part VI. Hydrogen bonding in simple and complex ammonium halides. *Canadian Journal of Chemistry*, *57*(4), 404–423. https://doi.org/10.1139/v79-068

Knop, O., Westerhaus, W. J., & Falk, M. (1980). Infrared spectra of the ammonium ion in crystals. Part VIII. Spectroscopic criteria of highly-bent hydrogen bonds. *Canadian Journal of Chemistry*, *58*(9), 867–874. https://doi.org/10.1139/v80-136

Knop, O., Westerhaus, W. J., Falk, M., & Massa, W. (1985). Infrared spectra of the ammonium ion in crystals. Part XIV. Hydrogen bonding and orientation of the ammonium ion in fluorides, with observations on the transition temperatures in cubic cryolite, elpasolite, and perovskite halides. *Canadian Journal of Chemistry*, *63*(9), 3328–3353. https://doi.org/10.1139/v85-551

Krohn, M. D., & Altaner, S. P. (1987). Near-infrared detection of ammonium minerals. *Geophysics*, *52*(7), 924–930. https://doi.org/10.1190/1.1442362

Madejovà, J., Gates, W. P., & Petit, S. (2017). IR spectra of clay minerals. In W. P. Gates, J. T. Kloprogge, J. Madejová, F. Bergaya (Eds.), *Infrared and Raman spectroscopies of clay minerals* (Vol. 8, pp. 1–604).

Marchi, S., Raponi, A., Prettyman, T. H., De Sanctis, M. C., Castillo-Rogez, J., Raymond, C. A., et al. (2019). An aqueously altered carbon-rich Ceres. *Nature Astronomy*, *3*(2), 140–145. https://doi.org/10.1038/s41550-018-0656-0

Petit, S., Richi, D., Madejova, J., & Decarreau, A. (1998). Layer charge estimation of smectites using infrared spectroscopy. *Clay Minerals*, *33*(4), 579–591. https://doi.org/10.1180/claymin.1998.033.4.05

Pironon, J., Pelletier, M., de Donato, P., & Mosser-Ruck, R. (2003). Characterization of smectite and illite by FTIR spectroscopy of interlayer NH4+ cations. *Clay Minerals*, *38*(2), 201–211. https://doi.org/10.1180/0009855033820089

Raponi, A., Carrozzo, F. G., Zambon, F., De Sanctis, M. C., Ciarniello, M., Frigeri, A., et al. (2019). Mineralogical mapping of Coniraya quadrangle of the dwarf planet Ceres. *Icarus*, *318*, 99–110. https://doi.org/10.1016/j.icarus.2017.10.023

Robinson, J. W. (1974). *CRC handbook of spectroscopy*. CRC Press.

Russell, C. T., Coradini, A., Christensen, U., De Sanctis, M. C., Feldman, W. C., Jaumann, R., et al. (2004). Dawn: A journey in space and time. *Planetary and Space Science*, *52*(5–6), 465–489. https://doi.org/10.1016/j.pss.2003.06.013

Russell, J. D. (1965). Infra-red study of the reactions of ammonia with montmorillonite and saponite. *Transactions of the Faraday Society*, *61*, 2284–2294. https://doi.org/10.1039/tf9656102284

Russell, J. D., & Farmer, V. C. (1964). Infra-red spectroscopic study of the dehydration of montmorillonite and saponite. *Clay Minerals Bulletin*, *5*(32), 443–464. https://doi.org/10.1180/claymin.1964.005.32.04

Russell, J. D., & White, J. L. (1966). Infrared study of the thermal decomposition of ammonium rectorite, clays and clay minerals. In *Proceedings of the Fourteenth National Conference, Berkeley, California* (pp. 181–191). https://doi.org/10.1016/b978-0-08-011908-3.50017-7

Salisbury, J. W., & Walter, L. S. (1989). Thermal infrared (2.5-13.5 μm) spectroscopic remote sensing of igneous rock types on particulate planetary surfaces. *Journal of Geophysical Research*, *94*(B7), 9192–9202. https://doi.org/10.1029/jb094ib07p09192

Yang, Y., Busigny, V., Wang, Z., & Xia, Q. (2017). The fate of ammonium in phengite at high temperature. *American Mineralogist*, *102*(11), 2244–2253. https://doi.org/10.2138/am-2017-6094

Yariv, S. (2001). IR spectroscopy and thermo-IR spectroscopy in the study of the fine structure of organo-clay complexes. In S. Yariv & H. Cross (Eds.), *Organo-clay complexes and interactions* (p. 680). CRC Press. https://doi.org/10.1201/9781482270945